NAVAL SHIP RESEARCH AND DEVELOPMENT CENTER

Washington, D.C. 20007

PRESSURE-VELOCITY RELATIONSHIP IN IMPACT OF A SHIP MODEL DROPPED ONTO THE WATER SURFACE AND IN SLAMMING IN WAVES

by

Margaret D. Ochi and
Jose' Bonilla-Norat

DEPARTMENT OF HYDROMECHANICS
RESEARCH AND DEVELOPMENT REPORT

June 1970

Report 3153

The Naval Ship Research and Development Center is a U.S. Navy center for laboratory effort directed at achieving improved sea and air vehicles. It was formed in March 1967 by merging the David Taylor Model Basin at Carderock, Maryland and the Marine Engineering Laboratory (now Naval Ship R & D Laboratory) at Annapolis, Maryland. The Mine Defense Laboratory (now Naval Ship R & D Laboratory) Panama City, Florida became part of the Center in November 1967.

Naval Ship Research and Development Center
Washington, D.C. 20007

MAJOR NSRDC ORGANIZATIONAL COMPONENTS

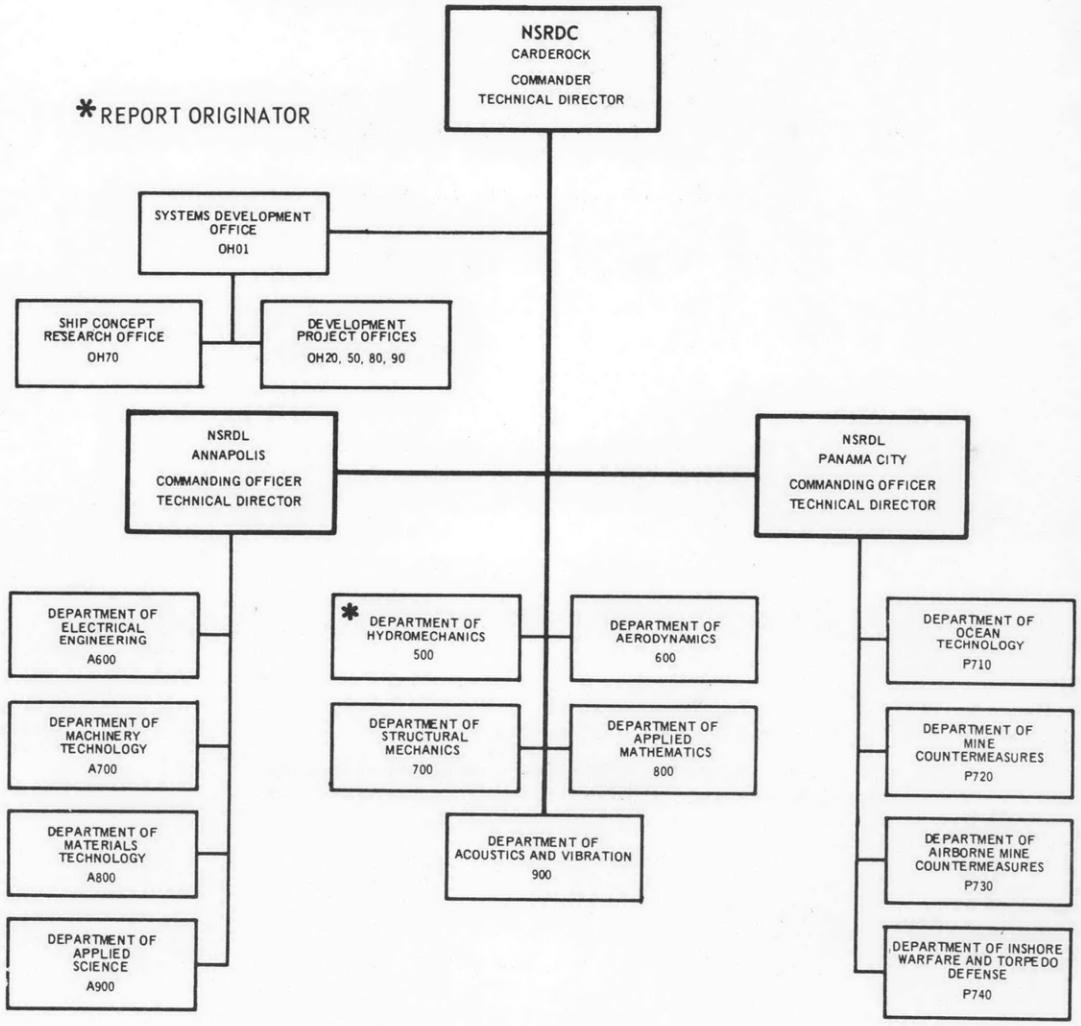

DEPARTMENT OF THE NAVY
NAVAL SHIP RESEARCH AND DEVELOPMENT CENTER
WASHINGTON, D. C. 20007

PRESSURE-VELOCITY RELATIONSHIP IN IMPACT OF A SHIP MODEL DROPPED ONTO THE WATER SURFACE AND IN SLAMMING IN WAVES

by

Margaret D. Ochi and
Jose' Bonilla-Norat

June 1970

Report 3153

TABLE OF CONTENTS

LIST OF FIGURES

LIST OF TABLES

ABSTRACT

An experimental study was carried out to correlate for various ship forebody shapes the impact pressure-velocity relationship as obtained by testing a model in waves and by dropping the model onto the water surface. It was found that both approaches yield pressures that are approximately proportional to the square of the impact velocity but that the drop tests yield pressures higher than those in waves by a factor of two to three for a given section shape. Both approaches yield the same qualitative results as to the relationship of pressure and section form; specifically, the more blunt the body, the larger the impact pressure for a given impact velocity.

ADMINISTRATIVE INFORMATION

This work was performed at the Naval Ship Research and Development Center (NSRDC) under the Naval Ship Systems Command (NAVSHIPS) RDT and E Program, General Hydromechanics Research, Subproject SR 009 01 01, Task 0100.

INTRODUCTION

The slamming (forward bottom impact) experienced by a ship navigating in rough seas not only poses a serious threat to its safe navigation but results in a considerable loss of time and money to the ship owner and operator as well. It is therefore highly desirable to develop the capability for estimating slamming impact loads while a ship is still in the design stage. The Ochi method[1] may be used for this purpose, but requires knowledge of the impact pressure-velocity relationship. Unfortunately, no adequate theory is available which will predict slamming pressures with any degree of certainty; at the present time therefore, the pressure characterization for any given form must be established experimentally. This has been pursued in two distinct phases. One is the two-dimensional approach consisting of the impact of a body onto the water surface; the other is the model experiment conducted in regular or irregular waves.

---

[1]References are listed on page 40

Studies to date have shown that the magnitude of impact pressure is a function of section shape and impact velocity only, but that for a given form and impact velocity, drop tests yield higher pressures than do model experiments in waves. The results of the latter type of tests are, of course, considered more meaningful.

Because seaworthiness tests are much more expensive to conduct than are drop tests, this present study was initiated to obtain information regarding correlation of the two approaches. It is a first step in an approach that, hopefully, will eventually lead to the characterization of the pressure-velocity-section shape relationship solely by means of drop tests. In this study, a MARINER model was tested in regular waves and the impact pressure-velocity relationship was obtained at three longitudinal locations. The model was then dropped from several heights and the pressure-velocity relationship due to impact with the free water surfact was obtained. The results for one section were also compared with those obtained from a drop of a two-dimensional constant section model of that station.[2]

METHOD

MODEL PARTICULARS

A 5.5-ft model of the MARINER was employed in these experiments. The characteristics of the model and the MARINER are given in Table 1 and the lines are shown in Figure 1. The model was ballasted to 40.4 percent of full load with a trim by stern of 0.57 in. The radius of gyration was established at 24.2 percent of the length between perpendiculars. The natural periods of pitch and heave (0.70 and 0.74 sec, respectively) were obtained by manually oscillating the model in these modes in calm water.

TEST PROCEDURE

Tests in Waves

The tests in waves were carried out in the NSRDC 140-ft basin in head regular waves generated by a pneumatic-type wavemaker. The model was towed under constant thrust by an electrically driven carriage which was run at a preset constant speed. The model was attached to a subcarriage

that was positioned on the main carriage and was free to travel fore and aft along a guide rail fixed to the main carriage, thereby permitting the model freedom in surge. The subcarriage was fitted with a heave staff which was free to travel on roller guides. The lower end of the staff was attached to the model center of gravity (CG) through a pivot connection, allowing the model freedom of motion in pitch and heave but restraining it in roll.

Thrust was provided by a gravity system in the low tow force range and by a magnetic clutch in the higher range (1.5 to 5.0 lb).

TABLE 1

Characteristics of MARINER

Item	Model	Prototype
Length LOA, ft	5.86	563.64
Length LBP, ft	5.50	528.00
Breadth B, ft	0.79	76.00
Depth D, ft	0.37	35.50
Draft max H_{max}, ft	0.31	29.75
Block coefficient C_b	0.624	0.624
Prismatic coefficient C_p	0.635	0.635
Midship coefficient C_x	0.983	0.983
Waterplane coefficient C_w	0.745	0.745
Displacement max ∇_{max}	51.5 (lb)	21,093 (ton)
Displacement light draft	32.3 (lb)	
Radius of gyration	0.242 L	0.24 L
Natural pitching period at light draft, sec	0.70	
Natural heaving period at light draft, sec	0.74	
Scale ratio	1	96.00

Table 2 indicates the experimental conditions for the slamming study. In wave length to ship length ratios (λ/L) of 1.0 and 2.0, tests were made over a large speed range and in waves ranging from mild to

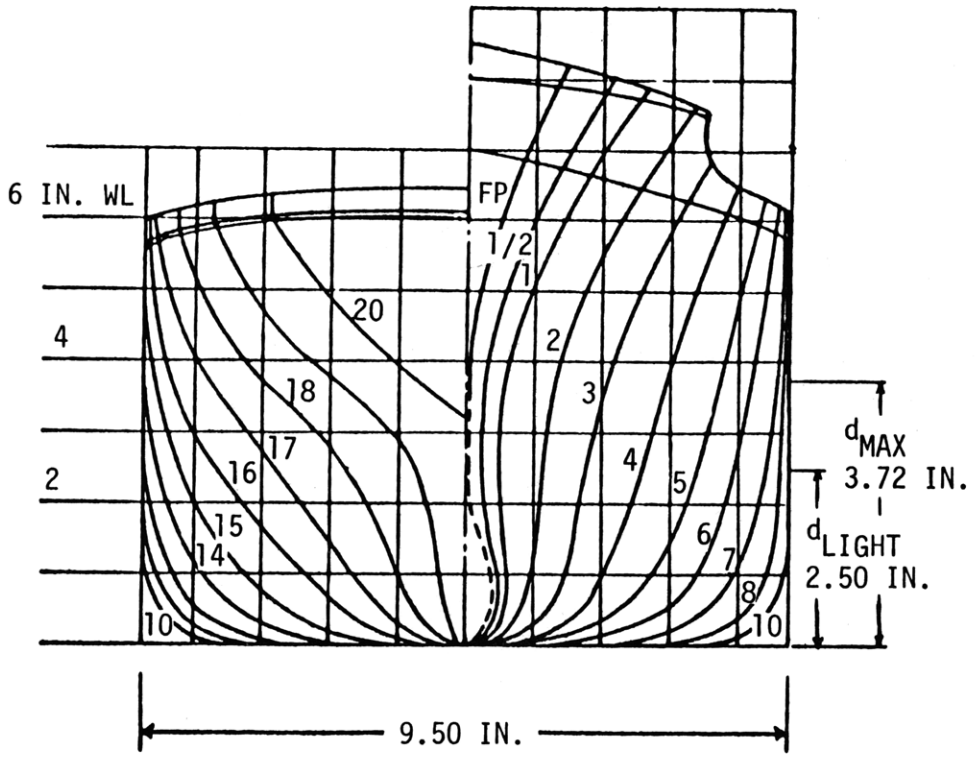

Figure 1 - Lines of MARINER Model

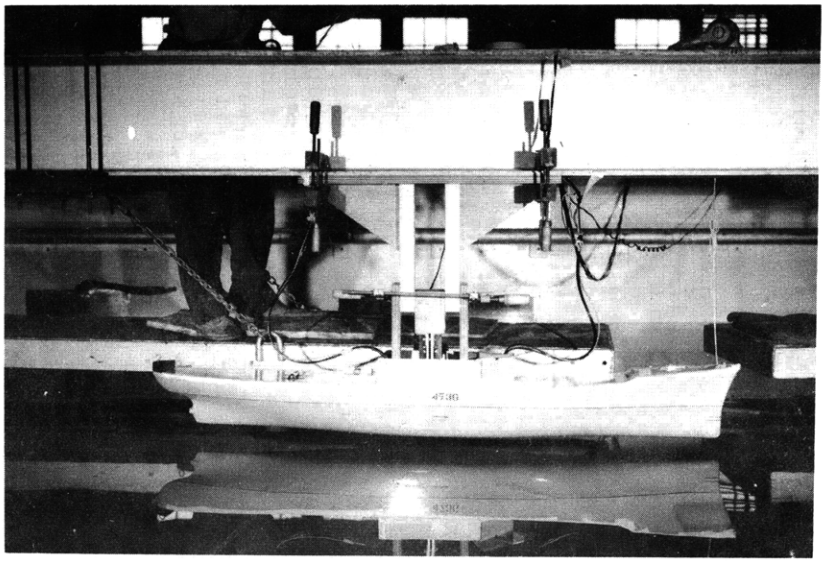

Figure 2 - Support Mechanism and Model
in Position for Drop Test

TABLE 2

Outline of Experimental Conditions

λ/L	λ/h Nominal	Ship Speed knots
1.00	20 to 60	0 to 30
1.25	40 20 to 60	0 20
1.50	40 30 to 60	10, 15 25
1.75	40	10, 15
2.00	20 to 60	0 to 30
2.25	40	10, 15

severe to provide sufficient data to establish the impact pressure-velocity relationship, and to determine to what extent, if any, ship speed and wave length per se influence the occurrence of slamming.

Drop Tests

The drop tests were carried out in the 60- by 22-ft NSRDC circulating water channel; a water depth of 9 ft was used for these tests. The drops were performed at the center of the tank and three-dimensional flow conditions were permitted. The support system for the model was attached to an I-beam running lengthwise along the midsection of the channel. It consisted of a block, adjustable for movement in the vertical direction, within supporting legs which were fixed to the I-beam. A quick release mechanism was affixed to the lower end of the block. The model was secured at a predetermined height by inserting a pin through a link of the quick release mechanism into a catch rod assembly installed in the model. Activation of a solenoid triggered the release mechanism and allowed free fall of the model. Figure 2 is a photograph of the apparatus with the model in position for release.

The model was dropped at heights ranging from 1.5 to 7.5 in. corresponding to velocities at impact of approximately 2.7 to 6.3 ft/sec. Drops were made onto a calm water surface. The effect of forward speed was examined by dropping the model first with no current in the channel and then with current velocities of 1.0 and 2.4 knots.

INSTRUMENTATION

Wave height, pitch and heave motions, bow accelerations, motion relative to the waves, and impact pressures along the keel over the forward 30 percent of the ship forebody were measured in the experiments. Pitch and heave were measured by potentiometers located on the tow staff of the subcarriage, and bow accelerations were obtained at Station 2 1/2 by a $\pm$2g Statham accelerometer. Wave dimensions were measured by a sonic probe mounted on the carriage and forward of the model.

Piezoelectric crystal pressure gages were located at Stations 2, 3, 3 1/2, and 5, and diaphragm-type transducers were utilized at Stations 4 and 6. The diameter of the crystal gages was 0.375 in. and that of the diaphragm gages was 0.5 in. The crystal gages had a flat response up to 40 kc and a 6-msec rise time. Acceleration sensitivity was 0.02 psig. The natural frequency of the diaphragm gages was 7000 cps.

Water elevation relative to the model was measured by resistance-type bow probes fitted around the model girth at Stations 2, 3 1/2, and 5. The output of the various sensors was fed through appropriate amplifiers. The ship motions and wave height were recorded on a direct-writing Sanborn Chart recorder and all pressures, bow acceleration, and relative motions were recorded by a CEC galvanometer oscillograph and datarite system. The overall response of the high frequency recording system was 1200 cps.

PRESENTATION AND DISCUSSION OF EXPERIMENTAL RESULTS

CHANGE IN LEVEL

Inasmuch as draft at the ship bow is an influential factor in the incidence of slamming, it is important to know the change in water level at the bow when the ship is underway. Accordingly, the model was first towed in calm water throughout the speed range of interest and the change in level along the model side was measured by the relative motion probes located at Stations 2, 3 1/2, and 5. The results are shown in the top graph of Figure 3. The change in water level ΔH (indicated by the solid lines) consisted of changes due to geometric position of the model relative to the undisturbed water surface as well as a rise of water because of the bow wave. The change in level at the bow due to trim and

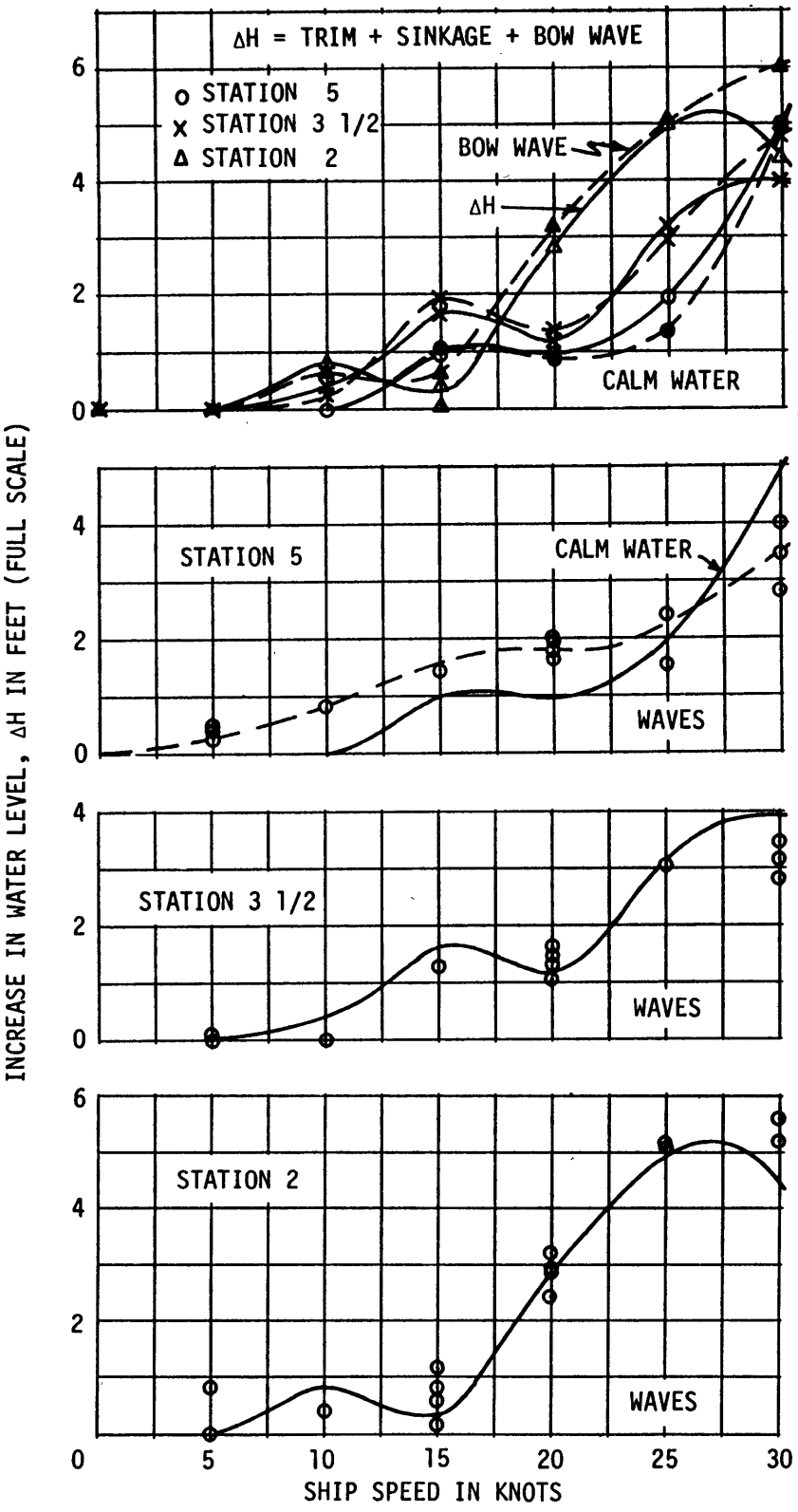

Figure 3 - Variation in Change of Level with Speed

sinkage (rise) was evaluated from the pitch and heave potentiometer measurements and this effect was subtracted, leaving only the bow wave contribution to the change in water level as shown by the dashed lines in the figure. Note that at all three stations there was virtually no change in level due to trim and sinkage up through a speed of 25 knots; some effect did appear at 30 knots at Stations 2 and 3 1/2. Thus within the speed range of practical interest, the rise of water above the static waterline for this hull form in ballast condition was due to the bow wave alone. For considerations of bow emergence (a prerequisite for slamming), effective draft underway may therefore be considered to be the ballast draft plus the height of the bow wave.

The rise of water at the model side due to the bow wave is speed-dependent and becomes considerable at the high speeds. At 25 knots, for example, the rise of water due to the bow wave at Station 2 amounted to 27 percent of the ballast draft. It is of interest to compare the change in water level obtained in calm water with that in waves; see the bottom three graphs of Figure 3. The solid lines represent the calm water change in level, and the wave data are indicated by the circles. In general there was good agreement between the change in level in waves and the calm water results at Stations 2 and 3 1/2. Although the general trend was preserved at Station 5, the change in level in waves was somewhat higher than that in calm water at speeds below 25 knots.

TESTS IN WAVES

Measured pitch and heave and their phases with the waves are summarized in Appendix A along with bow acceleration at Station 2 1/2. These data were used to compute the vertical motion along the ship length and the motion of the ship relative to the waves for selected test conditions using the Froude-Kriloff assumption that the structure of the wave is not influenced by the presence of the ship. Details of the computations are given in Appendix B. The results for vertical motion from Equation (B-1) of Appendix B are shown in Figure 4 in nondimensional form. The hyperbolic distribution of vertical motion along the ship length had a point of least motion occurring in the region of 52 to 65 percent of the ship length

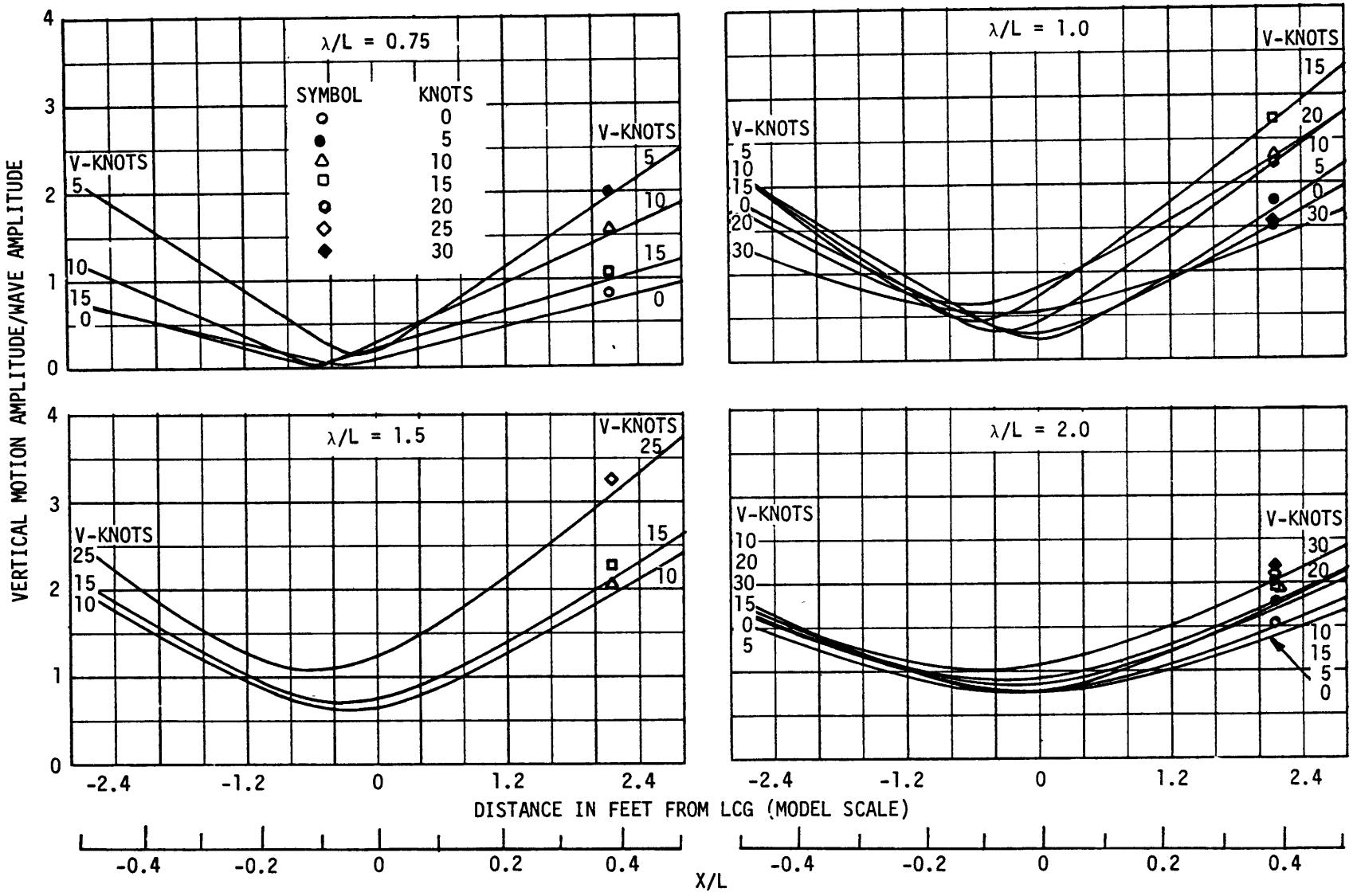

Figure 4 - Vertical Motion along Ship Length for Various Speeds

aft of the forward perpendicular depending on the particular wave length and speed. The position of this point of minimum motion along the ship length was influenced to a great extent by the phase between pitch and heave.

In any given wave length, the effect of speed on the vertical motion was greater over the forward part of the ship than over the aft portion, and motion at the stern was generally less and never greater than that at the bow.

The figure also includes the vertical motion at Station 2 1/2 (12.5 percent of LBP aft of the forward perpendicular (FP)) as determined from the accelerometer measurements. The agreement between measured values at this location and those computed from the pitch and heave was good for all wave lengths and speeds. This would indicate that the error introduced in the measurements due to angular movement of the accelerometer was minimal even in the comparatively severe conditions which induce slamming.*

The amplitude of relative motion between the ship and wave was computed from Equation (B-2). These results, nondimensionalized by the wave amplitude, are plotted along the ship length in Figure 5. Several interesting features are apparent from this figure:

1. Relative motion at the bow was greater than that at the stern for all wave lengths; this difference became more pronounced with an increase in speed.
2. In long waves ($\lambda/L = 2.0$), the amplitude of the relative motion exceeded the wave amplitude only at the foremost portion of the ship.
3. There were two locations along the ship length where the relative motion was minimal at speeds of 15 knots and below and only one minimum at speeds above 15 knots. The location of these minima shifted aft with increasing speed. As might be expected, the minima always occurred in the region where the ship motion was in phase with the wave motion.

---

*Note that these results were derived from data obtained in wave steepnesses $\lambda/2\zeta_A$ ranging from approximately 20 to 60.

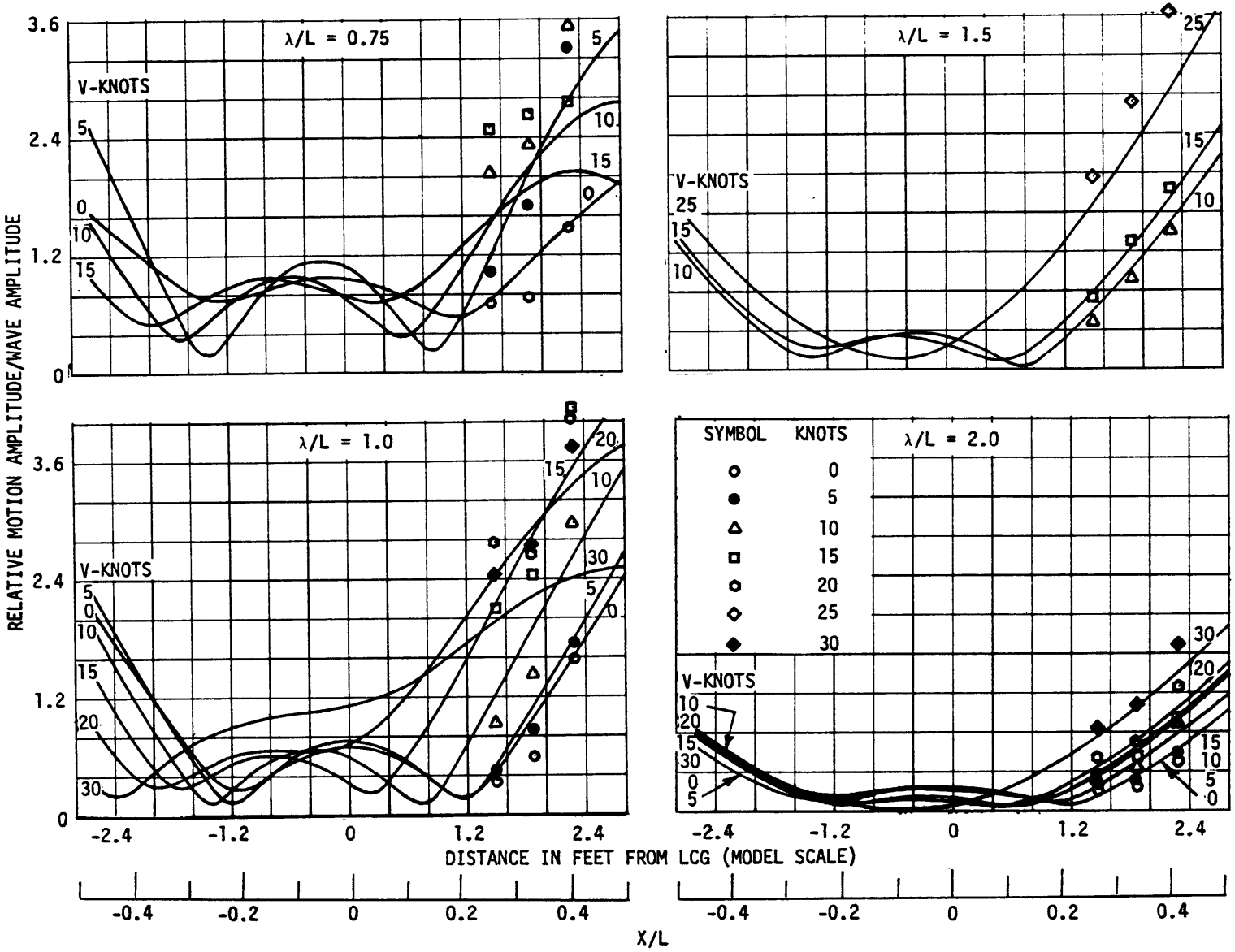

Figure 5 - Relative Motion along Ship Length for Various Speeds

The figure also includes the relative motion results as measured by the resistance wire probes located at Stations 2, 3 1/2, and 5.

Figure 6 presents another comparison of the measured and computed values for speeds of 0, 10, and 15 knots throughout the range of wave lengths tested. From Figures 5 and 6 the following comments may be made:

1. Agreement between measured values of relative motion and those computed from the pitch, heave, and wave was best for waves longer than the ship. The agreement was quite good in these wave lengths for speeds up through 15 knots.
2. In waves whose lengths were equal to or less than the length of the ship, the measured values were generally higher than those computed, and this discrepancy increased with speed. However, in $\lambda/L = 1.0$ the agreement may be considered adequate at speeds of 15 knots and below. Agreement was generally the poorest at Station 2, and the discrepancy was significant for high speeds; in the extreme cases, the computed values were in the order of only 70 percent of the measured values.

As mentioned earlier, the computational approach assumes that the ship does not produce changes in the surface of the surrounding water. In other words, in the evaluation of relative motion, the wave profile at the ship is considered to be that of the oncoming wave. Local disturbances to the wave introduced by the presence of the ship and by her motions as she pitches and heaves are neglected. On the other hand, the wire probe senses the change in water level at its location and consequently can include local effects in its measurement. Thus, the distortion of the wave due to forward speed as well as the superposition of the model-generated waves on the existing waves are reflected in the measured values. The effect of the former takes the form of a d-c shift or offset from the original zero about which the oscillations take place. Hence, this effect could be accounted for in the measured values of relative motion. However, the effect of the model-generated waves is included in the measured values. The discrepancy between the measured and computed values can, therefore, most probably be explained on this basis.

Grim[3] shows that the enlargement of the wave amplitude at the bow of a freely moving body is of the order of 20 to 25 percent in wave lengths

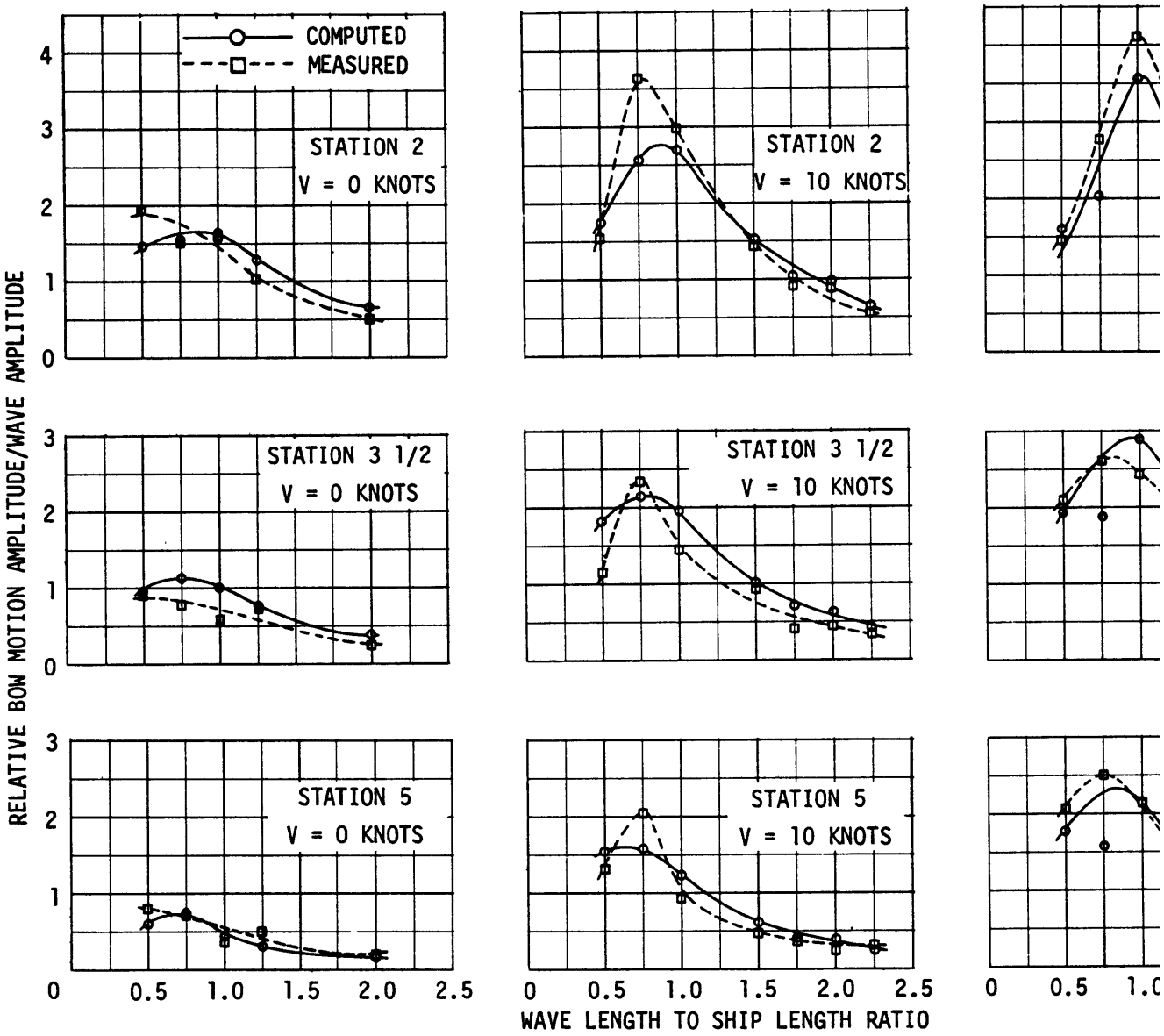

Figure 6 - Comparison of Measured and Computed Relative Motion at Stations 2, 3 1/2, and 5

λ/L = 1.0 to 1.5 at zero speed. Vladimirov[4] shows that at high Froude numbers (Fr=0.35), the rise in water level at the bow of a model oscillating in pitch can be as much as 100 percent. Tsai[5] shows that for the heaving of a two-dimensional body, a similar increase can be expected depending on body shape and frequency of oscillation. The cases in the present study where computed relative motion was only of the order of 70 percent of the measured value occurred at 20 knots in λ/L = 1.0, and an increase in wave height of about 100 percent would be required to yield the measured value. Although it cannot be said that the model-generated waves and the undisturbed wave system are necessarily additive, the above reported values of wave deformation are consistent with the trends found in relative motion measurements for the present study.

The phase between ship motion and wave motion over the length of the ship is shown in Figure 7. When the phase difference ($2\pi X/\lambda - \varepsilon_X$) was 180 deg, the two motions opposed each other; if it was 0 or 360 deg, the ship moved with the wave. The most critical case was, of course, the 180-deg out-of-phase condition where the downward moving ship met an upward moving wave. In waves greater than ship length, this critical condition was never reached even at the higher speeds; in waves of ship length and less, however, motions at the bow did approach the 180-deg out-of-phase condition at the higher speeds.

This figure provides some insight into why stern slamming is generally not a serious problem. For instance, the phase at the stern approached the 180-deg value only in waves shorter than the ship and then only in hove-to condition. This is not considered serious, however, since short waves will generally not have sufficient energy to cause appreciable motions of the ship. In wave length equal to ship length, a critical wave for motions, the phase was about 90 deg at zero speed and became more favorable with an increase in speed. At very high speeds, the stern motion was completely in phase with the wave motion. The change of phase with speed was only about 10 to 30 deg in the longer waves.

As mentioned earlier, the location along the ship length where the relative motion curves showed minima (see Figure 4) coincided with the location where these curves showed a zero phase difference.

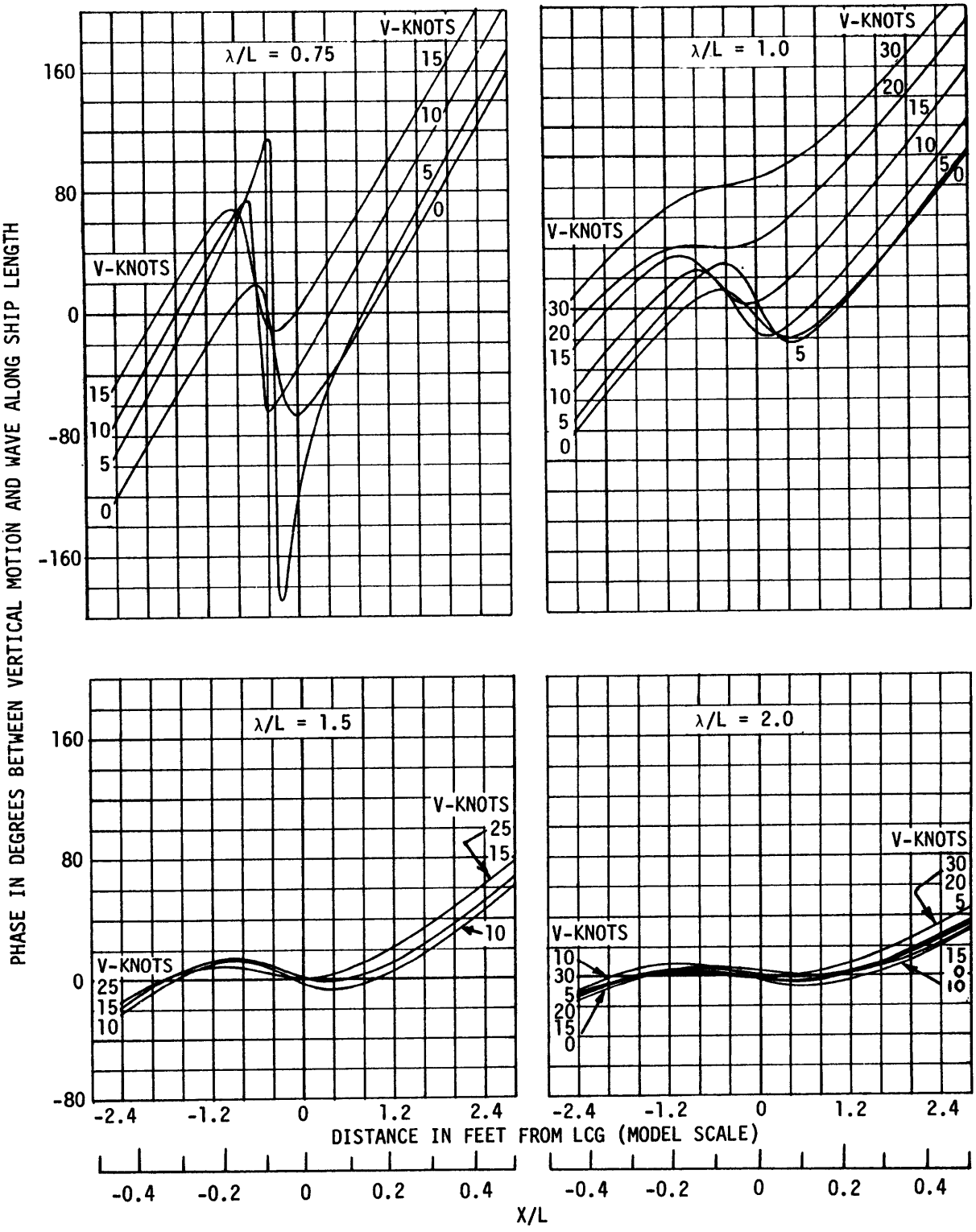

Figure 7 - Phase along Ship Length between Ship Motion and Wave

SLAMMING

Conditions Affecting Slamming

Slamming depends very strongly on the phase relation between wave motion and ship motion as well as on the magnitude of the relative velocity (motion) between ship and wave. It may therefore be of interest to examine these phases at a location along the ship length of interest for slamming and to determine how large a relative velocity may actually be expected. The data presented in Figure 8 pertains to Station 2. The location was selected on the basis of findings[6] that the presence of a pressure applied at 0.1L aft FP (Station 2) is a suitable indicator of the occurrence of a slam. Figure 8 indicates that speed had little effect on phases in long waves; the motions were only 20 to 30 deg out of phase with the waves throughout the speed range. In waves of the order of ship length, phases varied from about 70 deg at zero speed and increased sharply to the critical 180-deg out-of-phase condition at the higher speeds. The phases were most unfavorable in waves shorter than the ship, the most critical speeds being of the order of 10 to 15 knots.

The lower graph in Figure 8 shows the amplitude of relative bow velocity nondimensionalized by dividing by the product of the wave amplitude and the frequency of encounter. This presentation yields the response amplitude operator of the relative motion. The maximum unit relative motion was about 3.5, and this occurred in $\lambda/L = 1$ to 1.25 at speeds of 15 to 20 knots. In waves of $\lambda/h = 22$, amplitudes of relative motion would be approximately 40 to 50 ft full scale and relative velocity amplitudes about 40 to 45 ft/sec. At 5 knots, the largest unit relative motion occurred in waves shorter than the ship. This figure clearly indicates why slamming is critical for the MARINER at speeds of 15 to 20 knots in waves equal to ship length and why it is considerably relieved by reducing speed. At the 15- to 20-knot speed, the relative velocity was large and phases unfavorable. Decreasing speed not only reduced the relative velocity but also improved the phases. It may be of interest to mention that the synchronous speed for pitch for MARINER for this ballast draft condition in $\lambda/L = 1.0$ was 15 knots.

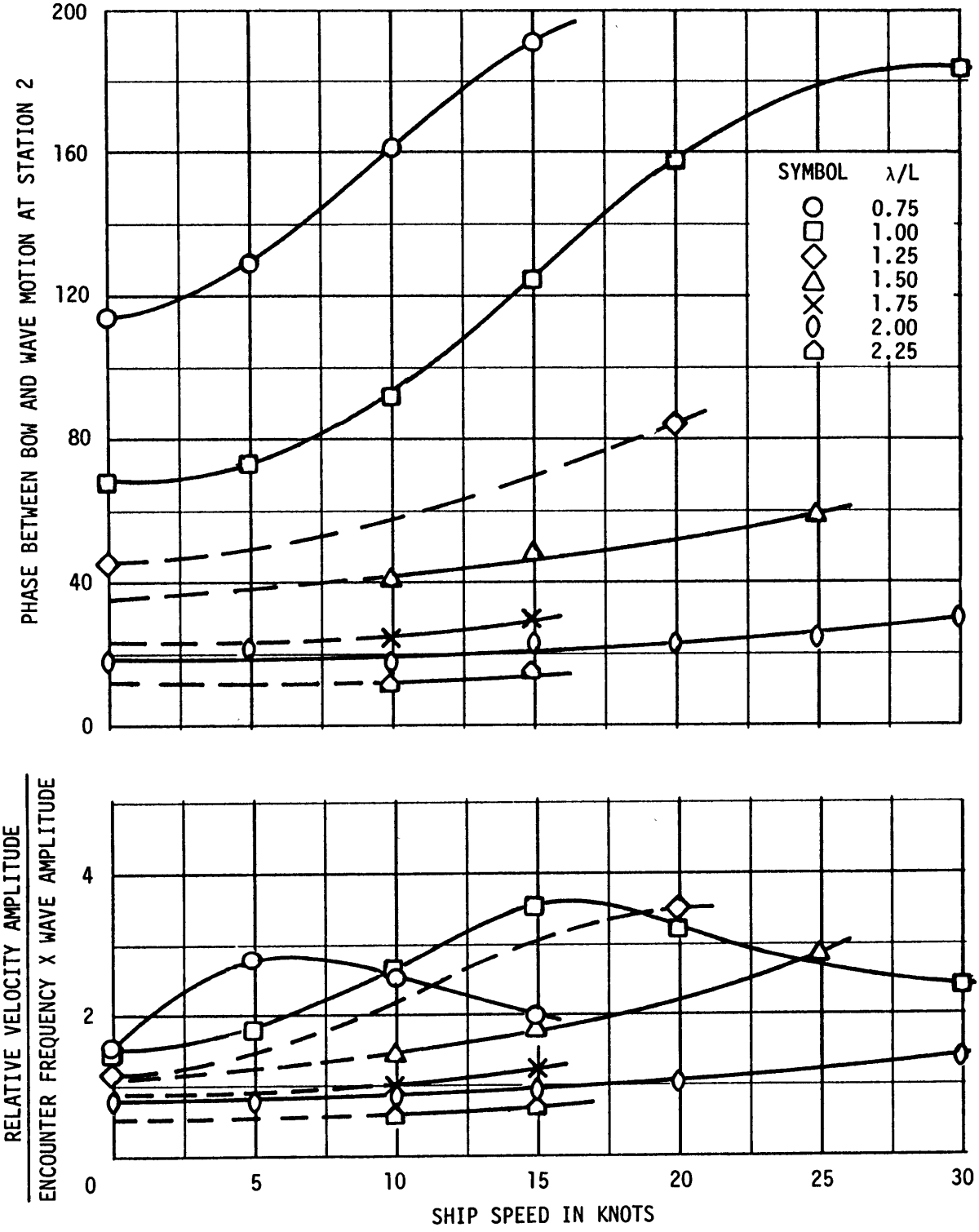

Figure 8 - Amplitude and Phase of Relative Motion at Station 2

Impact Pressures in Waves

As discussed in the previous section, the most severe slamming occurred in $\lambda/L = 1.0$. The peak pressures on the model occurring at speeds of 1.0, 1.5, 2.0, and 3.0 knots (10, 15, 20, 30 knots full scale) have been plotted in Figure 9 for various wave steepnesses. As expected, the pressure amplitudes increased with wave steepness. The maximum measured pressures correspond to about 125 psi for the full-scale ship. These occurred in the vicinity of 15 to 17.5 percent of the ship length aft of the FP at speeds of 15 and 20 knots.

A tendency for the pressures to shift aft with increasing speed was clearly evident. For example, at 2.0 and 3.0 knots, pressures occurred as far aft as 30 percent of the model length. This is most critical for the 2.0-knot speed where the pressure magnitudes remain relatively high over the forward 25 percent of the model length such that the combination of the high pressures and large surface area result in large forces applied to the hull bottom.

It may be of interest to compare the pressures measured in the present tests with those obtained in Reference 7. This comparison is shown in Figure 10 for $\lambda/L = 1.0$ at a constant wave steepness of $\lambda/h = 20$. The gage types were different in the two tests and so was the overall response of the recording systems, but the agreement between the two sets of data is considered remarkably good. The largest discrepancy occurred for Station 2; the earlier results were somewhat lower than those from the present tests. In general, however, both the trends and magnitudes repeated exceptionally well.

Peak pressures measured at Stations 2, 3 1/2, and 5 are plotted as a function of the measured impact velocity in Figures 11a, 12a, and 13a, respectively.* Since the data fall on a straight line when plotted on logarithmic scale, the pressures may be simply expressed in the form:

*Model-scale values are given in these and subsequent figures.

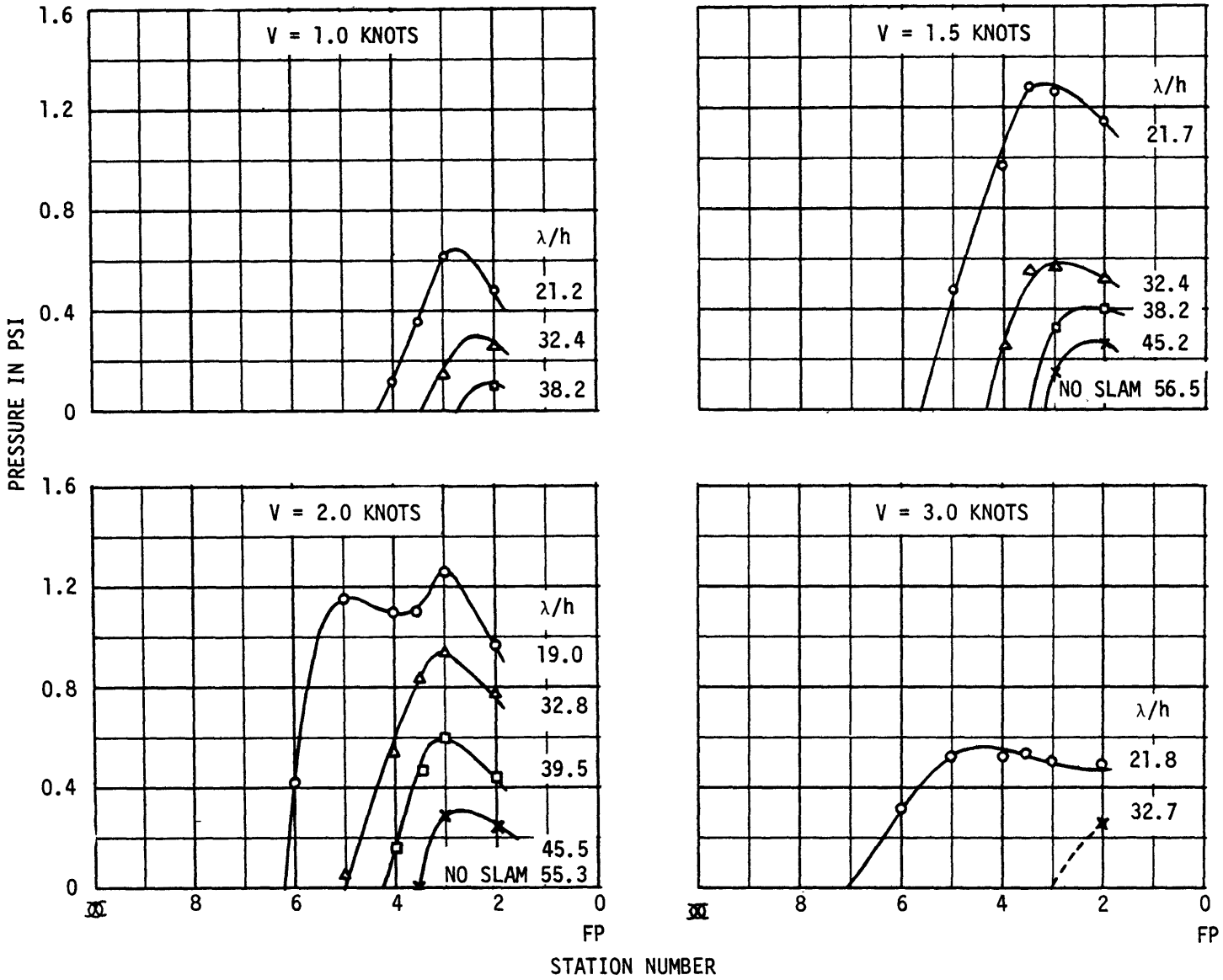

Figure 9 - Distribution of Slamming Pressure along Keel Line in Waves of $\lambda/L = 1.0$

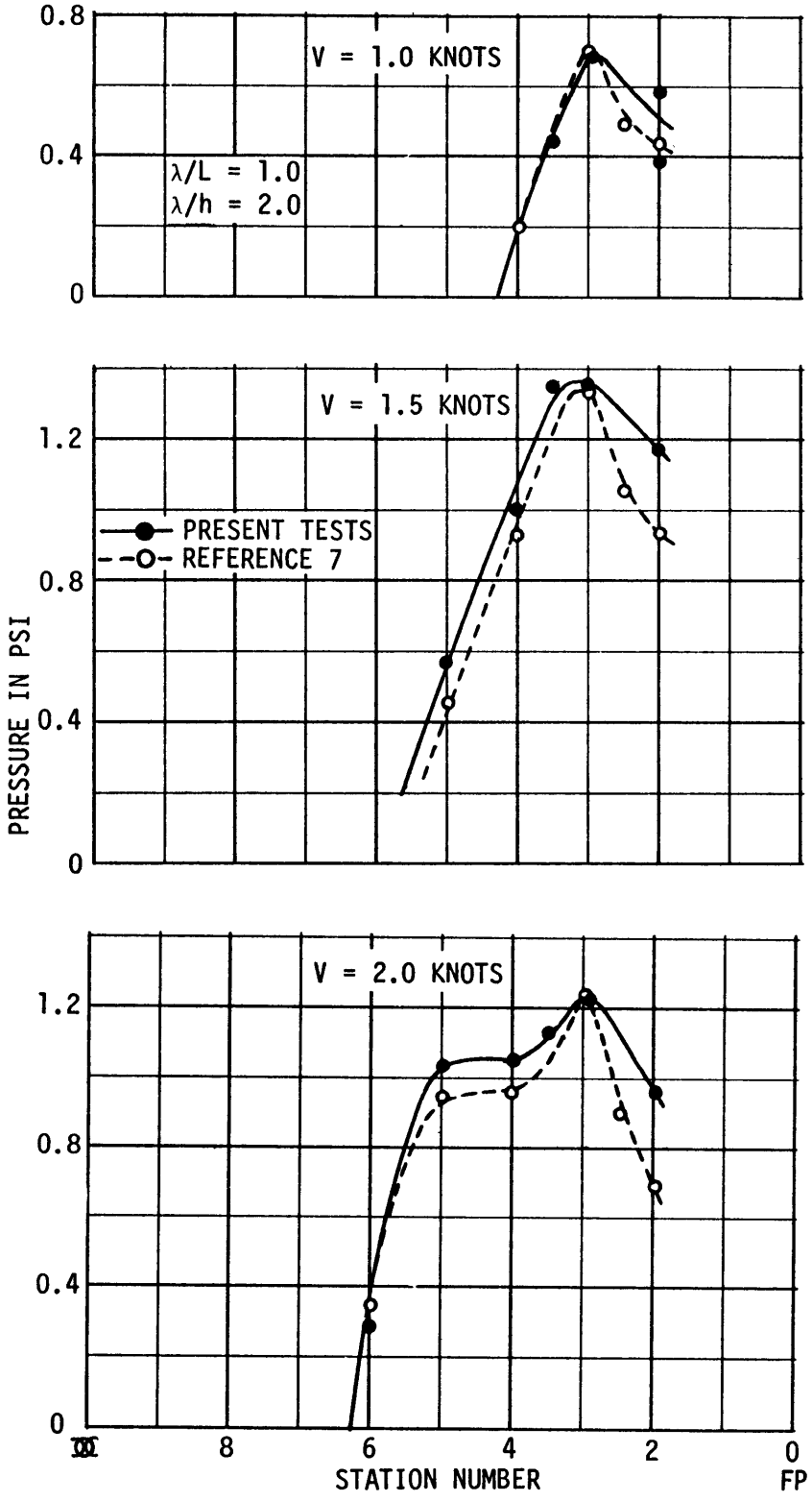

Figure 10 - Comparison of Pressures Obtained with Measuring Systems of Different Frequency Response Characteristics

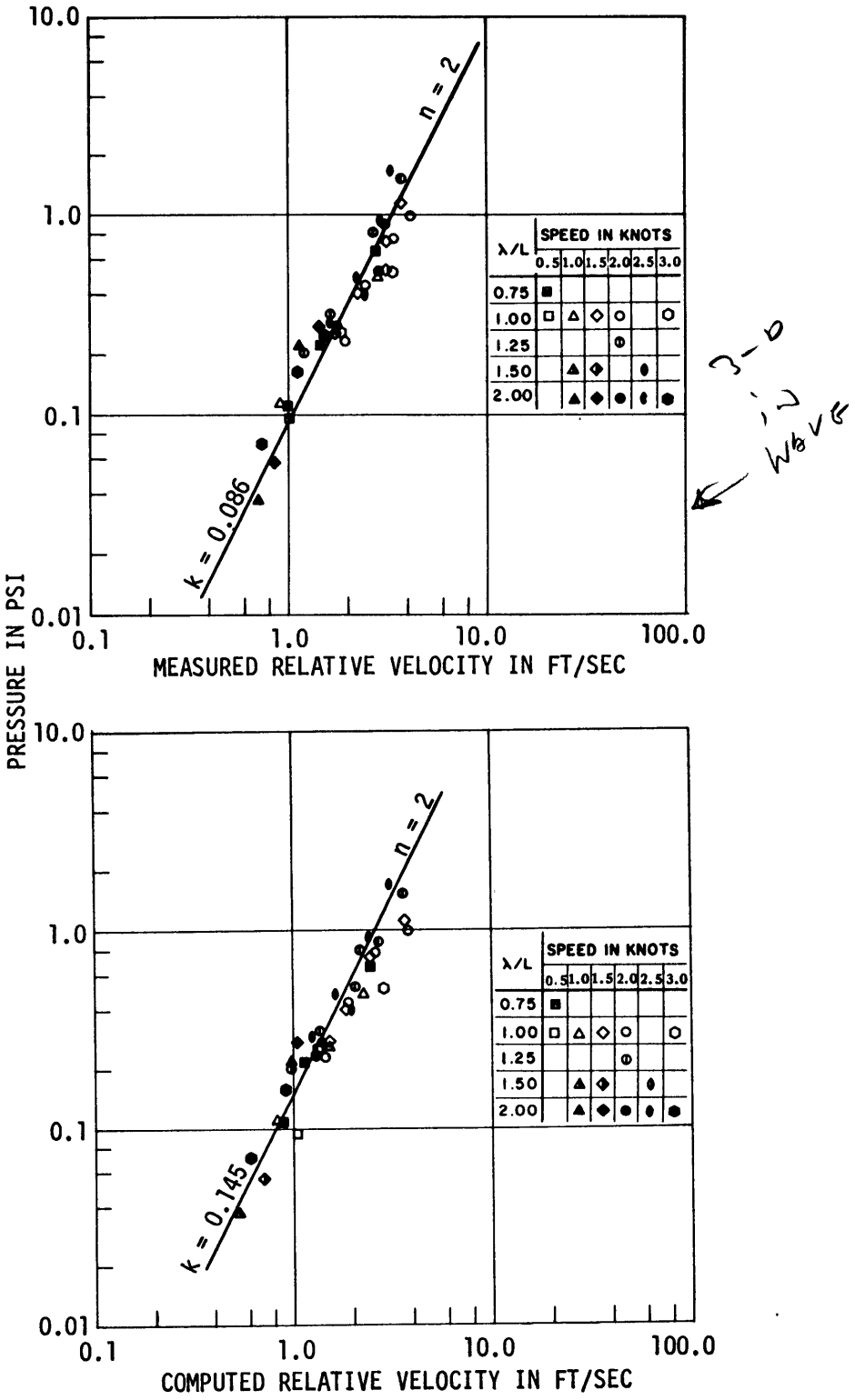

Figure 11 - Peak Pressure at Station 2 as a Function of Impact Velocity from Model Tests in Waves

$$p = kv^n$$

where p is the impact pressure,

v is the impact velocity, and

k and n are constants determined from the graph.

The lines in the figures have been drawn such that the pressure is proportional to the square of the velocity. Although this is not quite exact, the data indicate that the assumption of velocity squared is sufficiently close to justify its use because of convenience.

The constant k varies for the three stations depending on the shape of the particular section; specifically, the finer the sectional form, the smaller the value of k. However, it is apparent that the k-value is not a function of ship speed and that it is also independent of the wave conditions.

The measured pressures were also plotted as a function of the relative velocity evaluated from Equation (B-3) where the value of "t" at which the slam occurred was determined from the records. These results are shown in Figures 11b, 12b, and 13b. They tended to yield k-values somewhat higher than those determined from the measured velocities and this effect was most pronounced at Station 2. This difference is in accordance with what might be expected from the earlier discussion pertaining to the discrepancy in measured and computed relative motion. As pointed out there, the computed motions do not include the effect of attenuation of the wave profile as the wave progresses along the ship. The relative motion probe, however, senses the local wave profile and thus gives measured amplitudes larger than the computed values. This, in turn, is reflected in the relative velocity. Thus, for the same pressure magnitude, the computed velocities are generally smaller, resulting in the larger k-values in Part b of Figures 11 through 13.

It has been shown that pressure is proportional to the square of the velocity at impact and that the proportionality constant k is dependent on the section shape. In particular, shape of the bottom portion up to about 0.08 draft has been reported to be critical.[8] The k-values from Figures 11a through 13a are plotted in Figure 14 as a function of sectional

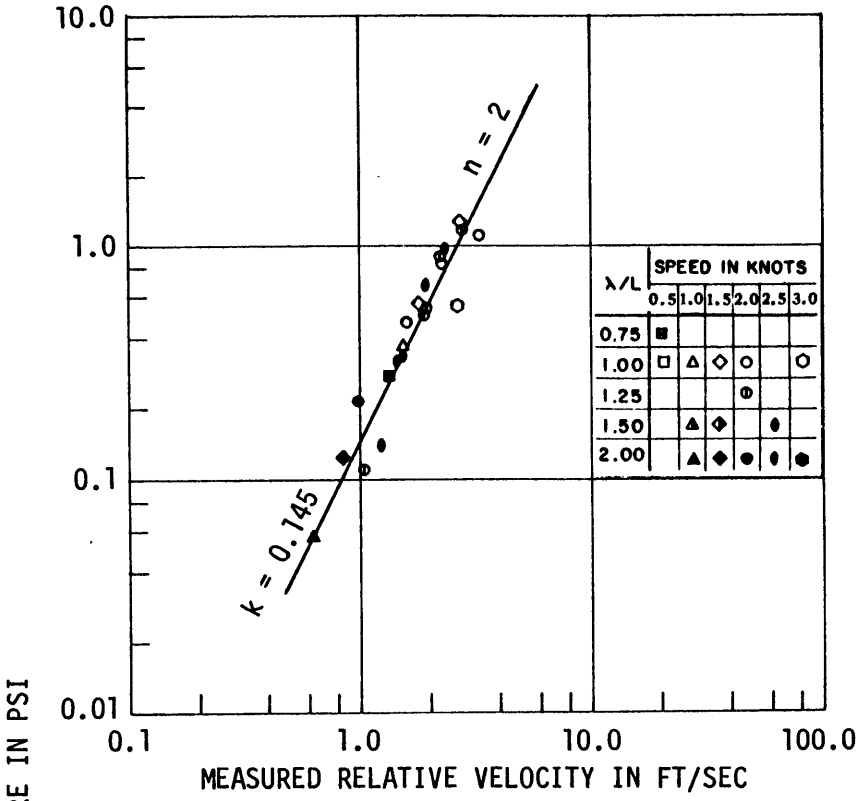

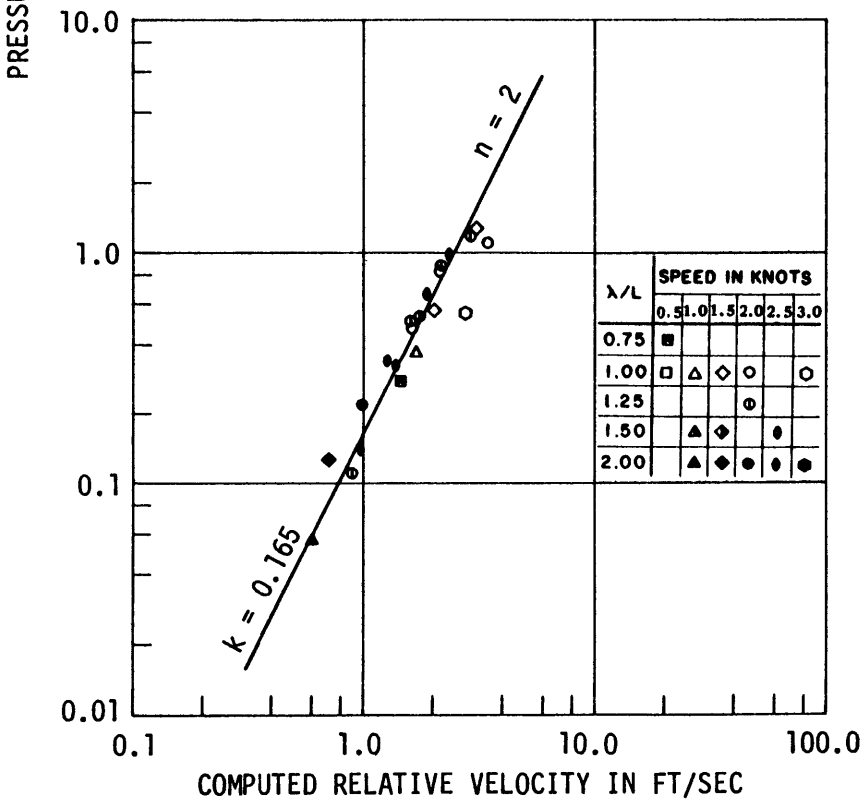

Figure 12 - Peak Pressure at Station 3 1/2 as a Function of Impact Velocity from Model Tests in Waves

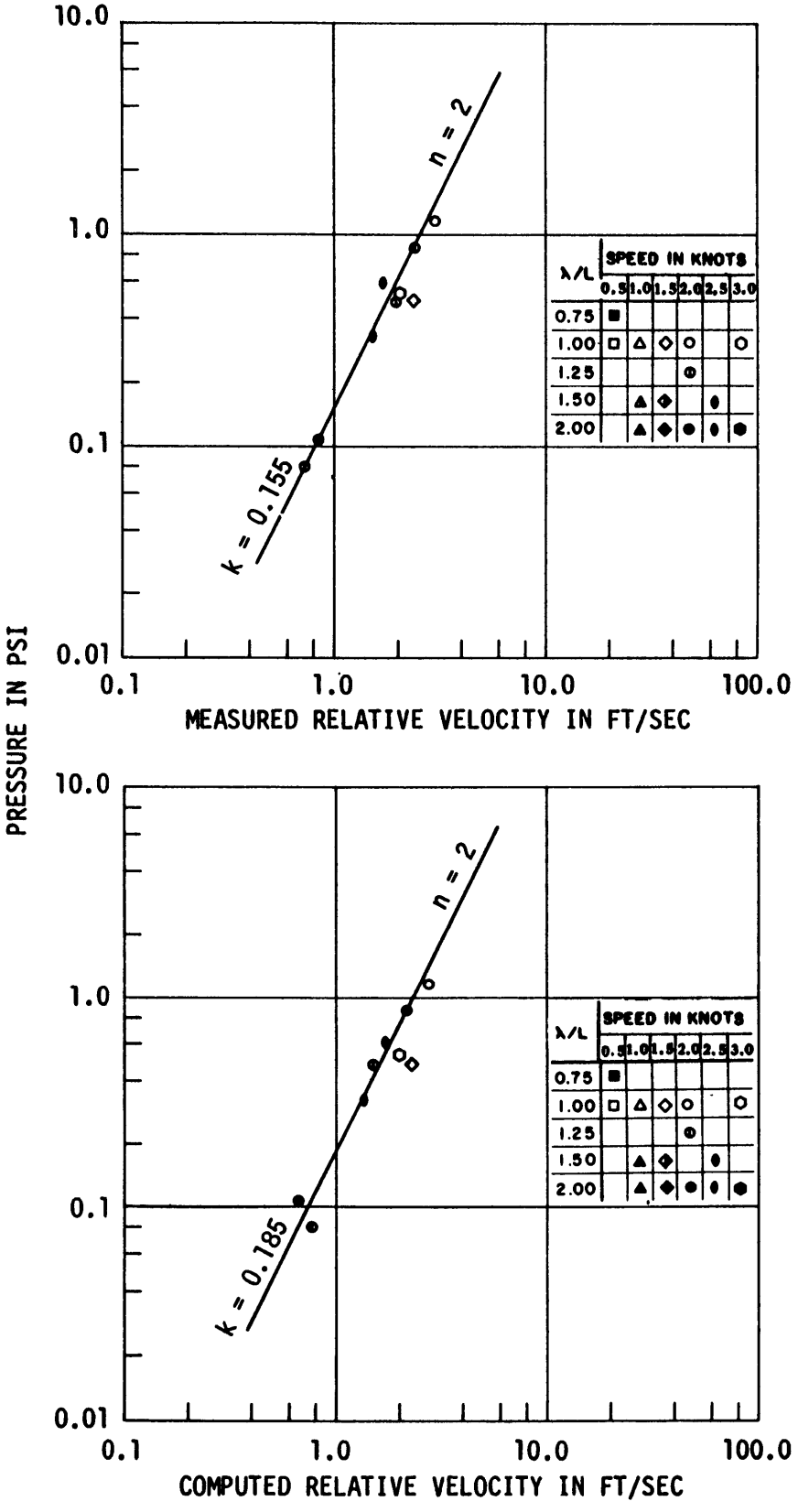

Figure 13 - Peak Pressure at Station 5 as a Function of Impact Velocity from Model Tests in Waves

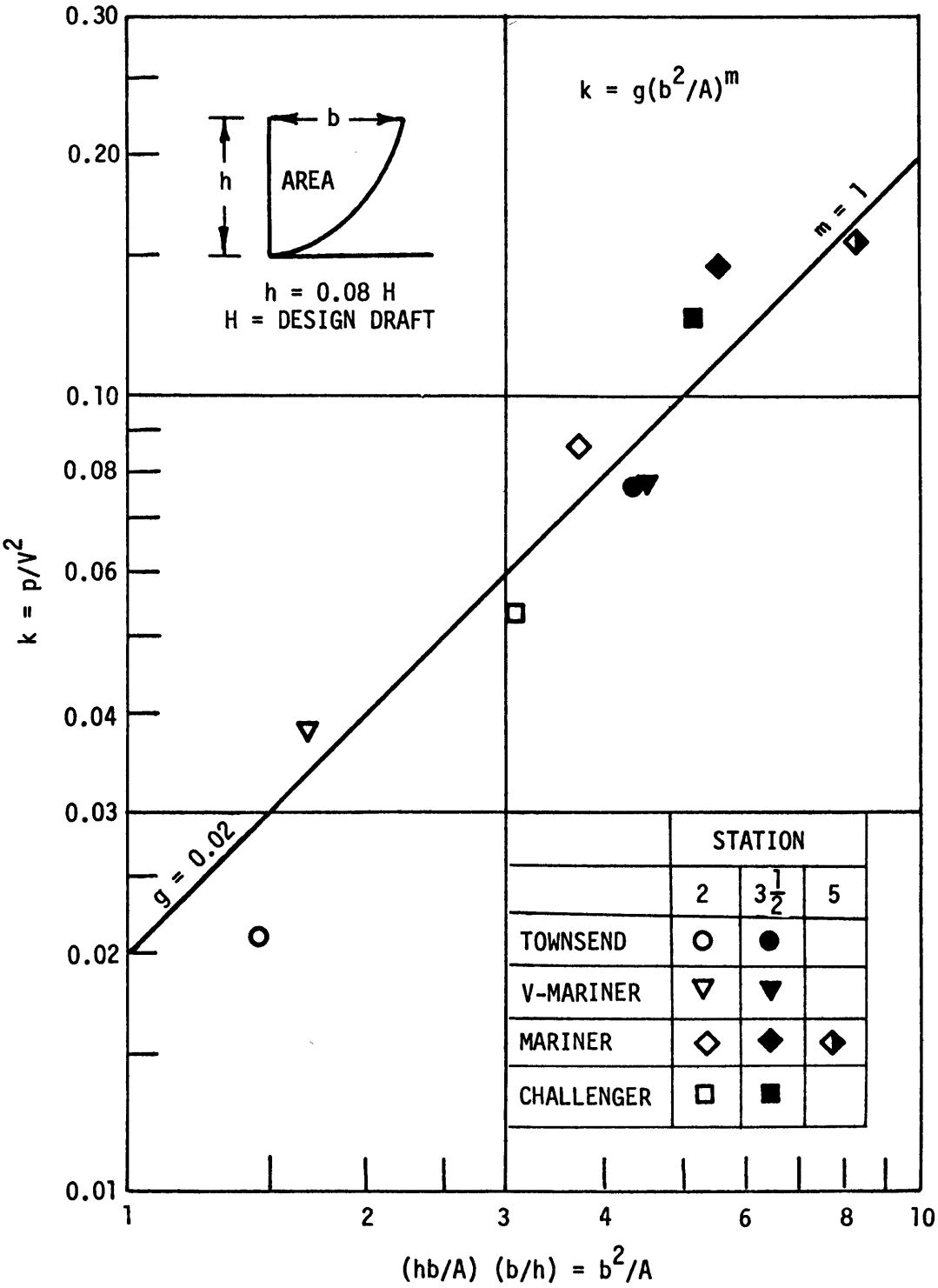

Figure 14 - k-Values for Various Section Forms

form defined by two parameters only. These are b/h ratios where b is the half-section breadth at h = 0.08 H (H is design draft) and the half-sectional area coefficient A/bh. Included also in the figures are data summarized in Reference 8 for other ship sections. From the straight-line relationship obtained when plotted on logarithmic scale, the k-value may be expressed in terms of sectional form as

$$k = 0.02 \frac{b^2}{A}$$

Hence the pressure becomes

$$p = 0.02 \frac{b^2}{A} V^2$$

where p is in pounds per square inch and V is in feet per second. The above formula simply expresses the peak pressure in terms of impact velocity and section shape. Although b^2/A represents a rather simplified measure of section shape, it may be useful for gross estimates of the order of magnitude of impact pressures which might be expected for a given ship sectional form. [For a more exact determination of k in terms of form parameters, the ship section should be expressed mathematically through conformal mapping techniques using sufficient terms to adequately fit the shape, and the k-values should be related to the coefficients of form through regression analysis. Such work is currently being carried out at the Center.]

Impact Pressure from Drop Tests

Figure 15 presents the peak pressures obtained from dropping the model in free fall onto a calm water surface from various heights (correspondingly, a series of impact velocities). The range of impact velocities investigated corresponded to about 25 to 60 ft/sec for the full-scale ship. The pressures are shown along the model length, and the corresponding flat bottom width at the appropriate longitudinal location is shown at the top of the figure. The plotted pressures represent the average of approximately ten drops at each height which resulted in flat impact. Since the model was not guided in its descent, it would at times

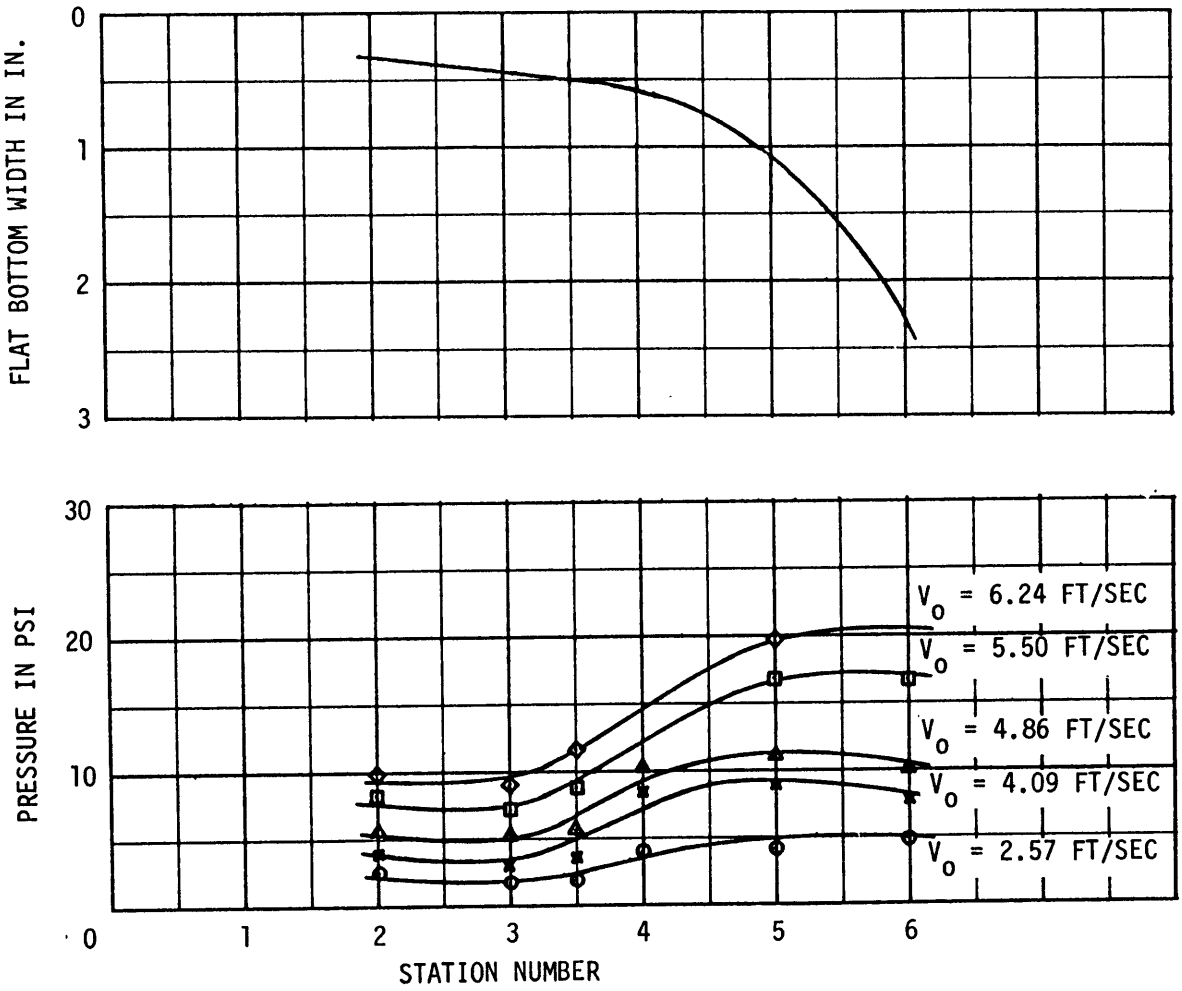

Figure 15 - Peak Pressure along MARINER Forebody for Various Impact Velocities from Three-Dimensional Drop Tests

impact with a slight angle of attack. Such conditions were detected by a time differential of impact from the foremost to the aftermost gage, and these were eliminated from the analysis. Figure 15 appears to indicate that the pressure magnitudes were significantly influenced by the extent of flat bottom over the forward 25 percent of the model length. Beyond the quarter length, between Stations 5 and 6, there was a marked increase in flat bottom but was not reflected in the pressure magnitude. This could suggest that air entrapment may become involved when the flat bottom increases beyond a certain amount.

Peak pressures as a function of impact velocity are indicated in Figure 16 together with the results obtained when the model was dropped onto a surface having a stream velocity of 1.0 and 2.4 knots. No discernible effect of forward velocity was apparent. This trend was in agreement with the model test results in waves. As was also the case in the seaworthiness tests, the peak pressures were approximately proportional to the square of the impact velocity. For the same impact velocity, however, the pressures for any particular station were larger than those obtained in the seaworthiness tests. The k-values for the two types of tests differed by a factor of two at Station 3 1/2 and by a factor of three at Stations 2 and 5.

Figure 17 was prepared to provide a comparison of k-values obtained for the same section shape (that at Station 3 1/2 of MARINER) under entirely different test conditions. The lowest curve was obtained from seaworthiness tests in regular waves of the 5.5-ft model for speeds ranging from 0.5 to 3.0 knots. The intermediate curve was obtained from the drop tests of the same model onto a calm water surface, and the highest curve was obtained from a drop test of a 1:20-scale, two-dimensional model of constant cross section. For all three test conditions, the pressure was approximately proportional to the square of the impact velocity; however, results for the two-dimensional drop tests were greater than the tests in waves by about a factor of five and those of the three-dimensional drop tests about twice those in waves. For ease of comparison, the k-values for the various sections obtained by the different test methods are summarized below:

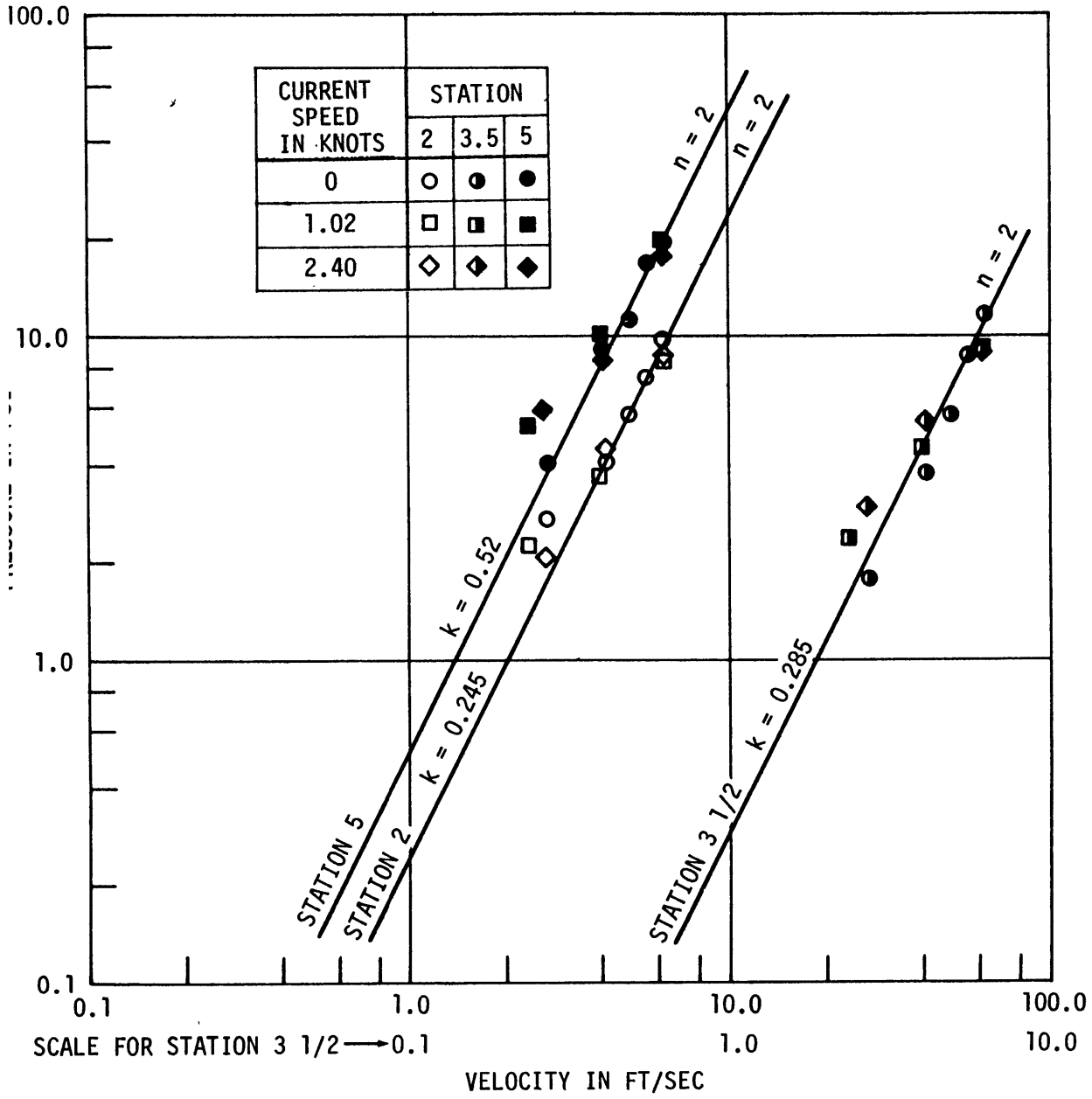

Figure 16 - Peak Pressure as a Function of Impact Velocity from Three-Dimensional Drop Tests

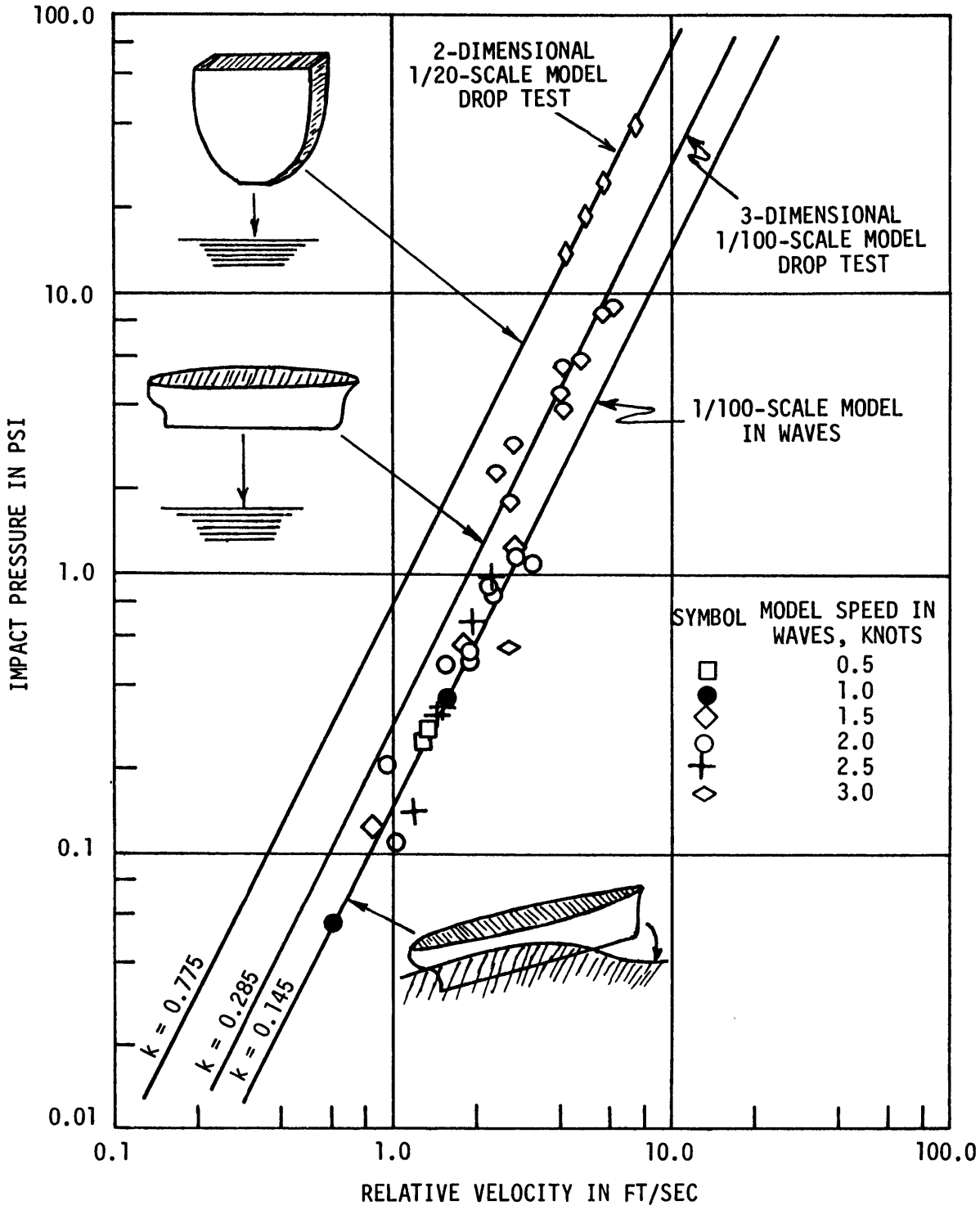

Figure 17 - Comparison of k-Values for Station 3 1/2 from Two- and Three-Dimensional Drop Tests and Tests in Waves

Section	$A/_{hb}$	Two-Dimensional Drop Tests	Three-Dimensional Drop Tests	Tests in Waves
Station 2	0.707		0.245	0.086
Station 3 1/2	0.765	0.775	0.285	0.145
Station 5	0.875		0.520	0.155

CONCLUSIONS

Tests to evaluate the correlation of impact pressures in ship slamming in waves with those obtained from drop tests were carried out on a 5.5-ft MARINER model. The motion characteristics and relative velocity in waves were also characterized. On the basis of these studies, the following conclusions are drawn:

1. There is no change in level for this hull form due to trim and sinkage for speeds up through 25 knots. However, the rise of water due to the bow wave can be as much as one-third of the ballast draft.
2. The location of minimum vertical motion along the ship length is in the region of 52 to 65 percent of the ship length aft of the FP.
3. At speeds below 15 knots, the relative motion is minimal at locations both forward and aft of amidship. These locations shift aft with speed. At speeds above 15 knots, there is only one minimum and this occurs well aft on the ship. The minima always occur in the region where wave and ship motion are in phase.
4. The relative motions computed from the pitch, heave, and nondeformed wave agreed reasonably well with the measured values for speeds up through 15 knots in waves of ship length or greater. For high speeds, however, in the region of $\lambda/L = 1.0$ to 1.5, the computed values were less; in the worst case, they were only about 70 percent of the measured values. This apparently resulted from the difference in the amplitude of the nondeformed surface wave as compared to that of the deformed wave in the region of the ship body.

5. Relative velocities between ship bow (Station 2) and wave can be as great as 40 to 45 ft/sec for MARINER in waves critical for slamming.
6. Maximum impact pressures were of the order of 125 psi full scale, and these occurred in the region of 15 to 17.5 percent of ship length aft of the FP at speeds of 15 to 20 knots in waves equal to ship length.
7. The impact pressures shift aft with speed and increased with wave height. No slamming occurred in waves $\lambda/2\zeta_A > 50$.
8. Impact pressures are approximately proportional to the velocity squared and the proportionality constant k is dependent on section shape; specifically, the finer the section, the smaller the k-value. This trend is borne out qualitatively by both the tests in waves and the drop tests although for a given impact velocity, the pressure is smaller for the seaworthiness tests than for the drop tests. Quantitatively the differences are in order of a factor of two to three for the three-dimensional drop tests and tests in waves. At Station 3 1/2, the results available from dropping a two-dimensional representation of that section indicate that the two-dimensional tests yield results greater than thests in waves by a factor of five.

RECOMMENDATIONS

1. Additional studies should be carried out to establish the extent to which the correlation factors between the drop tests and tests in waves apply to section shapes other than those investigated here.

2. The causes for the differences in the k-value as determined by three-dimensional drop tests and tests in waves should be more throughly investigated. Two factors which deserve consideration are the effects of surface waves and angle of impact.

ACKNOWLEDGMENTS

The authors express their appreciation to Mr. James Kallio for his participation in the design of the support system and release mechanism used in the drop tests. Thanks are also due to Messrs. I. Tonokawa and N. Milihram for their assistance with the instrumentation.

APPENDIX A
TABULATION OF BASIC MOTION AND WAVE DATA

Note: Bow acceleration is given in double amplitude.

λ/L	λ/ζ_w	$\theta_A/n\zeta_A$	Z_A/ζ_A	Bow Acceleration at Station 2 1/2 g	$\epsilon_{\theta\zeta}$	$\epsilon_{z\zeta}$	$\epsilon_{\theta\zeta}-\epsilon_{z\zeta}$	Wave Amp ζ_A in.	Test No.
Model Speed: 0 Knots									
0.5	14.7	0.085	0.156	0.293	189.5	171.0	18.5	1.125	113
0.75	15.2	0.177	0.089	0.333	89.2	66.8	22.4	1.625	85
	18.6	0.226	0.106	0.293	88.5	65.3	23.2	1.330	84
1.00	22.2	0.586	0.294	0.440	93.2	12.7	80.5	1.485	11
	33.7	0.550	0.250	0.259	92.1	6.1	86.0	0.980	13
	44.3	0.600	0.304	0.216	91.6	5.1	86.5	0.745	35
	50.0	0.652	0.311	0.208	86.1	3.7	82.4	0.660	26
	61.7	0.579	0.264	0.157	93.5	0.7	92.8	0.535	27
1.25	22.0	0.738	0.515	0.593	93.8	14.5	79.3	1.875	95
	38.7	0.783	0.502	0.316	89.6	3.6	86.0	1.065	97
2.00	20.6	0.885	0.777	0.474	92.3	2.9	89.5	3.200	45
	33.0	0.966	0.788	0.293	89.6	- 2.7	92.3	2.000	50
	36.8	0.934	0.769	0.276	83.4	- 8.8	92.2	1.795	66
	43.6	0.930	0.752	0.215	84.5	- 6.2	90.8	1.515	57
	55.5	1.056	0.761	0.172	84.8	- 3.1	87.9	1.190	73
Model Speed: 0.5 Knots									
0.75	18.4	0.546	0.203	0.944	58.0	94.8	-36.8	1.348	88 & 89
	27.1	0.552	0.185	0.734	72.7	133.7	-61.0	0.915	87
	31.7	0.549	0.236	0.577	59.7	118.4	-58.7	0.780	90
	36.1	0.557	0.166	0.479	84.5	150.8	-66.3	0.685	86
1.00	21.2	0.695	0.216	0.748	82.0	5.6	76.4	1.558	10 & 12
	35.3	0.700	0.267	0.460	96.8	- 5.7	102.5	0.935	14
	38.6	0.616	0.276	0.338	88.9	- 9.3	98.2	0.855	39
	50.8	0.730	0.235	0.362	91.8	-11.8	103.6	0.650	20
	61.7	0.694	0.277	0.240	80.7	-12.4	93.1	0.535	28
2.00	21.3	0.914	0.781	0.751	88.6	9.2	79.4	3.105	44
	33.0	1.004	0.818	0.430	82.1	- 2.5	84.7	2.000	49
	36.0	0.948	0.771	0.368	78.3	- 4.4	82.7	1.835	65
	43.3	0.987	0.780	0.313	79.7	- 2.2	81.9	1.525	56
	53.4	0.963	0.753	0.251	76.5	- 5.1	81.6	1.235	72
Model Speed: 1.0 Knots									
0.50	35.4	0.016	0.078	0.094	90.7	87.3	3.4	0.466	112
0.75	40.2	0.367	0.294	0.479	39.2	36.8	2.4	0.615	83
1.00	21.4	0.739	0.487	1.166	73.5	22.9	50.6	1.540	8 & 9
	32.4	0.830	0.479	0.841	67.3	15.4	51.9	1.020	15
	38.4	0.788	0.413	0.675	66.4	16.6	49.8	0.860	34
	44.3	0.804	0.379	0.609	59.5	14.4	45.1	0.745	21
	57.4	0.789	0.390	0.468	59.5	13.8	45.7	0.575	29
1.50	38.5	1.007	0.658	0.551	76.3	3.2	73.1	1.285	77
1.75	38.1	0.858	0.838	0.460	82.3	3.6	78.7	1.515	79
2.00	21.4	1.088	0.774	0.988	87.2	1.9	85.3	3.080	43
	33.6	1.193	0.888	0.538	86.9	5.5	81.4	1.965	48
	37.6	1.182	0.768	0.515	79.8	3.4	76.4	1.755	63 & 64
	44.3	1.184	0.768	0.391	83.4	4.4	79.0	1.490	55
	54.5	1.152	0.760	0.319	76.8	- 5.2	82.0	1.210	71
2.25	39.3	1.060	0.934	0.450	91.5	3.1	88.4	1.890	81

λ/L	λ/ζ_w	$\theta_A/n\zeta_A$	Z_A/ζ_A	Bow Acceleration at Station 2 1/2 g	$\epsilon_{\theta\zeta}$	$\epsilon_{z\zeta}$	$\epsilon_{\theta\zeta}-\epsilon_{z\zeta}$	Wave Amp ζ_A in.	Test No.
Model Speed: 1.5 Knots									
0.50	40.7	0.013	0.089	0.110	67.1	67.4	- 0.3	0.405	111
0.75	40.7	0.239	0.216	0.421	11.2	- 2.4	13.6	0.615	82
1.00	21.7	0.735	0.819	1.679	27.5	-18.4	45.9	1.520	7
	31.4	0.884	0.781	1.223	32.0	- 7.2	39.2	1.050	16
	38.2	0.847	0.658	0.988	36.3	- 1.0	37.3	0.865	33
	45.2	0.904	0.689	0.900	35.1	- 0.1	35.2	0.730	22
	56.7	0.910	0.630	0.727	35.7	1.5	34.2	0.582	30
1.50	38.1	1.074	0.750	0.754	70.7	- 1.1	71.8	1.300	76
1.75	38.8	1.084	0.789	0.643	78.2	1.9	76.3	1.490	78
2.00	20.8	0.966	0.844	1.165	86.9	3.7	83.2	3.175	42
	33.2	1.068	0.889	0.675	82.3	2.0	80.3	1.990	47
	37.4	1.060	0.864	0.580	79.2	- 1.0	80.2	1.768	62 & 63
	44.8	1.099	0.878	0.479	81.4	3.8	77.6	1.472	53 & 54
	54.9	1.083	0.856	0.389	78.5	- 1.5	80.0	1.202	69 & 70
2.25	38.1	1.047	0.890	0.509	82.5	1.0	81.5	1.950	80
Model Speed: 2.0 Knots									
1.00	20.8	0.600	0.831	1.741	2.6	-59.5	62.1	1.588	1,2,3,4
	32.8	0.742	0.896	1.340	9.6	-37.8	47.4	1.005	17
	39.6	0.764	0.826	1.115	10.8	-33.8	44.6	0.835	36 & 37
	45.2	0.768	0.829	1.027	10.6	-34.8	45.4	0.730	25
	56.4	0.788	0.803	0.822	9.6	-28.4	38.0	0.585	31
1.25	24.1	0.976	1.202	1.916	44.2	-14.0	58.2	1.710	94
	33.8	1.165	1.139	1.501	47.0	- 5.7	52.7	1.220	93
	38.7	1.190	1.052	1.323	53.1	0.6	52.5	1.065	96
	43.7	1.261	1.053	1.213	48.2	- 1.5	49.7	0.945	92
	55.0	1.313	1.027	0.958	47.8	- 2.1	49.9	0.750	91
	63.0	1.366	1.046	0.900	52.6	4.1	48.5	0.655	98 & 99
2.00	21.2	1.023	0.926	1.373	83.4	5.2	78.2	3.112	40 & 41
	33.0	1.122	0.898	0.822	79.2	2.5	76.7	2.000	51
	37.7	1.124	0.926	0.760	73.8	- 1.6	75.4	1.750	67
	44.4	1.135	0.916	0.592	79.5	0.5	79.0	1.488	58 & 59
	55.0	1.140	0.908	0.502	78.0	- 1.1	79.1	1.200	74
Model Speed: 2.5 Knots									
1.50	29.5	1.233	1.367	1.837	55.5	- 5.5	61.0	1.675	105
	35.9	1.352	1.283	1.565	57.7	- 2.5	60.2	1.380	104
	44.2	1.403	1.210	1.291	62.3	0.2	62.1	1.120	103
	50.0	1.422	1.187	1.144	61.5	0.4	61.1	0.990	102
	63.6	1.466	1.174	0.919	63.3	2.3	61.0	0.778	100 & 101
2.00	21.0	1.134	0.975	1.560	77.2	3.2	74.0	3.150	46
Model Speed: 3.0 Knots									
1.00	21.6	0.426	0.504	1.688	- 8.0	-90.0	82.0	1.535	5 & 6
	32.8	0.464	0.582	1.266	-13.6	-88.4	74.8	1.005	18 & 19
	40.0	0.462	0.573	1.027	-13.8	-84.0	70.2	0.825	38
	46.8	0.450	0.543	0.866	-16.6	-82.4	65.8	0.705	23 & 24
	56.4	0.446	0.552	0.685	-10.8	-78.8	68.0	0.585	32
2.00	32.8	1.142	1.084	1.223	72.3	3.2	69.1	2.015	52
	37.5	1.134	1.068	1.091	72.7	- 1.7	74.4	1.760	68
	44.3	1.172	1.084	0.890	71.3	0.8	70.5	1.490	60
	55.5	1.162	1.067	0.717	71.0	0.7	70.3	1.190	75

APPENDIX B

COMPUTATIONAL DETAILS OF BOW MOTION RELATIVE TO WAVES

Motions of a ship in head seas are considered. The problem then is that of a rigid body moving in the vertical plane with three degrees of freedom. Figure B1 depicts the plane motion of a ship. Fixed axes in space are designated x,z with the x-axis located in the undisturbed water surface. The origin of the body axes is at the center of gravity, and body axes are established by a right-handed coordinate system with the x-axis positive in the direction of the ship bow. Vertical motion of the LCG is defined as heave and is positive downwards. Pitch is zero when the waterplane is parallel to the undisturbed water surface and is positive for bow up. The heaving and pitching motions are represented by:

$$z = z_A \cos (\omega_e t + \varepsilon_{z\zeta})$$

and

$$\theta = \theta_A \cos (\omega_e t + \varepsilon_{\theta A})$$

The phase angles $\varepsilon_{z\zeta}$ and $\varepsilon_{\theta\zeta}$ are referred to the instant when the wave crest is at the longitudinal center of gravity (LCG). Positive $\varepsilon_{z\zeta}$ means heave leads wave, and positive $\varepsilon_{\theta\zeta}$ means pitch leads wave.

The vertical displacement at any point X along the ship is given by:

$$z_X = z - X\theta$$

where X is measured from LCG, positive forward
or

$$z_X = z_A \cos (\omega_e t + \varepsilon_{z\zeta}) - X\theta_A \cos (\omega_e t + \varepsilon_{\theta\zeta})$$

which can be written as

$$z_X = (z_X)_A \cos (\omega_e t + \varepsilon_{X\zeta})$$

where

$$(z_X)_A = \sqrt{z_A^2 + (X\theta_A)^2 - 2 z_A \theta_A X \cos (\varepsilon_{\theta\zeta} - \varepsilon_{z\zeta})} \qquad \text{(B-1)}$$

and $$\varepsilon_{X\zeta} = \tan^{-1} \frac{z_A \sin \varepsilon_{z\zeta} - X\theta_A \sin \varepsilon_{\theta\zeta}}{z_A \cos \varepsilon_{z\zeta} - X\theta_A \cos \varepsilon_{\theta\zeta}}$$

$\varepsilon_{\theta\zeta} - \varepsilon_{z\zeta}$ is the phase between pitch and heave and is positive if pitch leads heave; $\varepsilon_{X\zeta}$ is the phase between motion at point X and wave at LCG.

The value of X for which $(z_X)_A$ is minimum is

$$X_{min} = + \frac{z_A}{\theta_A} \cos (\varepsilon_{\theta\zeta} - \varepsilon_{z\zeta})$$

and

$$(z_X)_A \text{ min} = z_A \sin (\varepsilon_{\theta\zeta} - \varepsilon_{z\zeta})$$

The wave at the LCG is given by

$$\zeta = \zeta_A \cos \omega_e t$$

Hence the wave at point X is

$$\zeta_X = \zeta_A \cos \left\{ \frac{2\pi X}{\lambda} + \omega_e t \right\}$$

The position of point X relative to the waves is given by

$$p_X = \zeta_X + z_X$$

or

$$p_X = \zeta_A \cos \left\{ \frac{2\pi X}{\lambda} + \omega_e t \right\} + (z_X)_A \cos \left\{ \omega_e t + \varepsilon_{X\zeta} \right\}$$

which can be written as

$$p_X = (p_X)_A \cos (\omega_e t + \varepsilon_{p\zeta})$$

where $$(p_X)_A = \sqrt{\zeta_A^2 + (z_X)_A^2 + 2\zeta_A (z_X)_A \cos\left\{\frac{2\pi X}{\lambda} - \varepsilon_{X\zeta}\right\}} \qquad \text{(B-2)}$$

and $$\varepsilon_{p\zeta} = \tan^{-1} \frac{\zeta_A \sin \frac{2\pi X}{\lambda} + (z_X)_A \sin \varepsilon_{X\zeta}}{\zeta_A \cos \frac{2\pi X}{\lambda} + (z_X)_A \cos \varepsilon_{X\zeta}}$$

Here $\left[\frac{2\pi X}{\lambda} - \varepsilon_{X\zeta}\right]$ is the phase between the vertical motion at point X and the wave motion at that point and $\varepsilon_{p\zeta}$ is the phase between the relative motion at point X and the wave at the LCG. A vectorial representation of the motions is given in Figure B2.

The relative velocity becomes

$$\dot{p}_X = - \omega_e (p_X)_A \sin (\omega_e t + \varepsilon_{p\zeta}) \qquad \text{(B-3)}$$

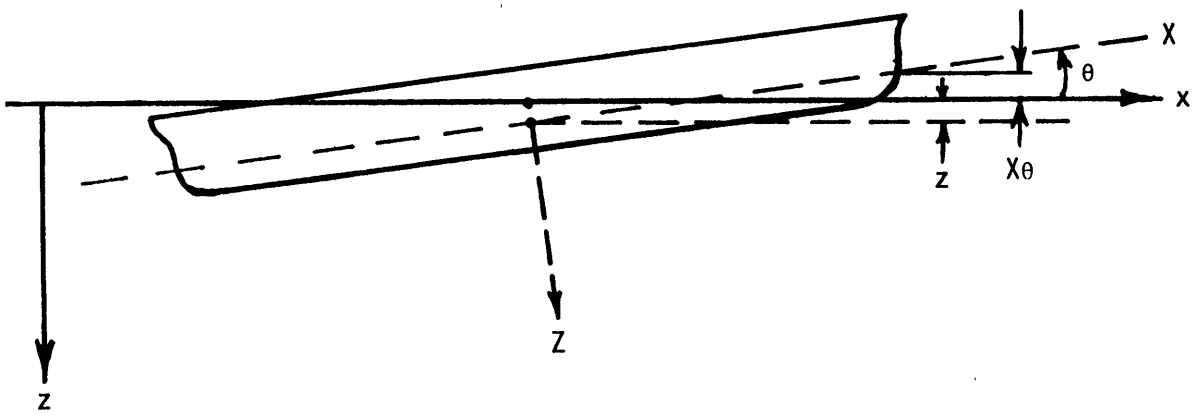

Figure B1 - Depiction of the Plane Motion of a Ship

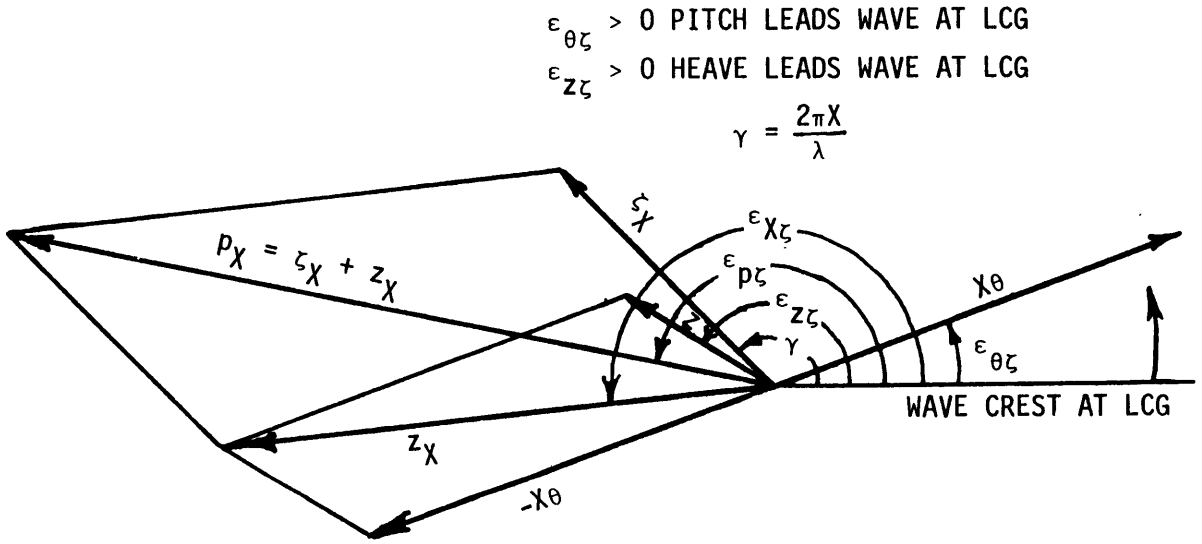

Figure B2 - Vectorial Representation of Motions

REFERENCES

1. Ochi, M.K., "Prediction of Occurrence and Severity of Ship Slamming at Sea," Presented at the Fifth Symposium on Naval Hydrodynamics, Bergen, Norway (Sep 1964).

2. Ochi, Margaret, D. and Schwartz, Frank, M., "Two-Dimensional Experiments on the Effect of Hull Form on Hydrodynamic Impact," David Taylor Model Basin Report 1994 (May 1966).

3. Grim, O., "A Method for a More Precise Computation of Heaving and Pitching Motions Both in Smooth Water and in Waves," Third Symposium on Naval Hydrodynamics, Scheveningen, Holland (Sep 1960).

4. Vladimurov, A.N., "Submersion of a Ship's Bow Under Head-on Waves," David Taylor Model Basin Translation 284 (Jan 1959).

5. Tsai, F., "Measurement of the Wave Height Produced by the Forced Heaving of Cylinders," Reports of Research Institute for Applied Mechanics, Vol VIII, No. 29 (1960).

6. Ochi, Michel, K., "Extreme Behavior of a Ship in Rough Seas," Translations, Society of Naval Architects and Marine Engineering (1964).

7. Ochi, Kazuo, "Model Experiments on the Effect of a Bulbous Bow on Ship Slamming," David Taylor Model Basin Report 1360 (Oct 1960).

8. Ochi, Michel, K., "Ship Slamming-Hydrodynamic Impact between Waves and Ship Bottom Forward," Symposium on Fluid-Solid Interaction American Society of Mechanical Engineers, Pittsburgh, Pa (1967).

INITIAL DISTRIBUTION

Copies	
1	NRL, Attn: Technical Info Div
4	NAVSHIPSYSCOM 2 SHIPS 2052 1 SHIPS 031 1 SHIPS 03412
6	NAVSEC 2 SEC 6110 2 SEC 6120 1 SEC 6132 1 SEC 6136
1	Naval Material Command 1 MAT 03L4
1	CNO, OP 07T (Tech Lib)
1	NASL
1	DNL
1	Commandant Chief Testing & Development Div, U.S. Coast Guard
1	Sci & Technical Div Lib of Congress
1	Nat'l Sci Foundation Engr Div
1	Chief Div of Ship Design Maritime Adm
1	Secretary, SNAME
1	American Bureau of Shipping 45 Broad St New York, N.Y. 10004
1	MIT, Attn: Dr. A.H. Keil
1	USN PostGraduate School Monterey, Calif 93940
1	Director Dept of Naval Architecture College of Engr Univ of Calif Berkeley, Calif 94720

Copies	
2	Webb Institute Crescent Beach Road Glen Cove, N.Y. 11542 1 President 1 Prof Walter Maclean
2	SWRI, 8500 Culebra Road San Antonio, Texas 78228 1 Dr. H.N. Abramson 1 Dr. C.R. Gerlach
1	The Univ of Michigan Dept of Engr Mechanics Ann Arbor, Michigan 48105
1	Director Experimental Naval Tank Willow Run Labs Box 2008 Ann Arbor, Michigan 48105
1	Director, Davidson Lab SIT
20	DDC

☆ U.S. GOVERNMENT PRINTING OFFICE: 1970-397-177/219

UNCLASSIFIED

Security Classification

DOCUMENT CONTROL DATA - R & D

(Security classification of title, body of abstract and indexing annotation must be entered when the overall report is classified)

1 ORIGINATING ACTIVITY (Corporate author)	2a. REPORT SECURITY CLASSIFICATION
Naval Ship Research and Development Center Washington, D.C. 20034	2b. GROUP

3 REPORT TITLE

PRESSURE-VELOCITY RELATIONSHIP IN IMPACT OF A SHIP MODEL DROPPED ONTO THE WATER SURFACE AND IN SLAMMING IN WAVES

4. DESCRIPTIVE NOTES (Type of report and inclusive dates)

5. AUTHOR(S) (First name, middle initial, last name)

Margaret D. Ochi and Jose' Bonilla-Norat

6. REPORT DATE	7a. TOTAL NO. OF PAGES	7b. NO. OF REFS
June 1970	44	8

8a. CONTRACT OR GRANT NO.	9a. ORIGINATOR'S REPORT NUMBER(S)
b. PROJECT NO. Subproject SR 009 01 01	3153
c. Task 0100	9b. OTHER REPORT NO(S) (Any other numbers that may be assigned this report)
d.	

10. DISTRIBUTION STATEMENT

This document has been approved for public release and sale; its distribution is unlimited.

11. SUPPLEMENTARY NOTES	12. SPONSORING MILITARY ACTIVITY
NAVSHIPS RDT and E Program, General Hydromechanics Research	NAVSHIPS

13. ABSTRACT

An experimental study was carried out to correlate for various ship forebody shapes the impact pressure-velocity relationship as obtained by testing a model in waves and by dropping the model onto the water surface. It was found that both approaches yield pressures that are approximately proportional to the square of the impact velocity but that the drop tests yield pressures higher than those in waves by a factor of two to three for a given section shape. Both approaches yield the same qualitative results as to the relationship of pressure and section form; specifically, the more blunt the body, the larger the impact pressure for a given impact velocity.

14 KEY WORDS	LINK A		LINK B		LINK C	
	ROLE	WT	ROLE	WT	ROLE	WT
Ship motions						
Hydrodynamic impact						
Slamming						
Drop tests						
Hull form effect						
Relative velocity						